Research Article Open Access

Combination of vitamins A, D2 and D3 reduce tumor load and alter the expression of miRNAs that regulate genes involved with apoptosis, tumor suppression, and the epithelial-mesenchymal transition in HCT-116 colon cancer cells

Karen D. Garay Buenrostro*[1], Keila C. Ostos Mendoza*[1], Pinal N. Kanabar*[2], Nina S. Los*[3], Temitope O. Lawal[4], Shitalben M. Patel[5], Alice M. López[6], Paulina Cabada-Aguirre[6], Nishikant A. Raut[5], Mark Maienschein-Cline[7], Zarema Arbieva[8], Gail B. Mahady[#5]

[1]School of Medicine and Health Sciences, Tecnológico University de Monterrey Monterrey, N.L., México and Department of Pharmacy Practice, College of Pharmacy, University of Illinois at Chicago, Chicago, IL, USA; [2]Research Informatics Core, Research Resources Center, University of Illinois at Chicago, Chicago, IL, USA; [3]Core Genomics Facility, Research Resource Center, University of Illinois at Chicago, Chicago, IL, USA; [4]Schlumberger Fellow, Department of Pharmacy Practice, University of Illinois at Chicago, Chicago, IL, USA and Department of Pharmaceutical Microbiology, University of Ibadan, Ibadan, Nigeria; [5]Department of Pharmacy Practice, College of Pharmacy, World Health Organization Collaborating Centre for Traditional Medicine, University of Illinois at Chicago, Chicago, IL, USA; [6]Department of Chemistry and Nanotechnology, Tecnológico University de Monterrey, Monterrey, Mexico and Department of Pharmacy Practice, College of Pharmacy, University of Illinois at Chicago, [7]Research Informatics Core, Research Resources Center, University of Illinois at Chicago, Chicago, IL, USA; [8]Core Genomics Facility, Research Resource Center, University of Illinois at Chicago, Chicago, IL, USA.

*These co-authors contributed equally to the work.

***Corresponding author:** Gail B. Mahady, Department of Pharmacy Practice, College of Pharmacy, World Health Organization Collaborating Centre for Traditional Medicine, University of Illinois at Chicago, Chicago, IL, 60612 USA

Submission Date: March 27th, 2022; **Acceptance Date:** April 12th, 2022; **Publication Date:** May 17th, 2022

Please cite this article as: Arbieva Z., Cabada-Aguirre P., Garay Beunrostro K. D., Kanabar P.N., Lawal T. O., Lopez A. M., Los N. S. Maienschein-Cline M., Ostos Mendoza K.C., Patel S. M., Raut N. A., Mahady G. B.. Combination of vitamins A, D2 and D3 reduce tumor load and alter the expression of miRNAs that regulate genes involved with apoptosis, tumor suppression, and the epithelial-mesenchymal transition in HCT-116 colon cancer cells. Functional Foods in Health and Disease. 2022; 12 (5): 216-241. DOI: https://www.doi.org/10.31989/ffhd.v12i5.925

ABSTRACT

Introduction: In previous work, we have shown the synergistic effects of combinations of vitamins A, D2, and D3 in reducing the proliferation of HCT-116 colon cancer cells. This combination also induced apoptosis and altered gene expression patterns as determined by transcriptomic profiling.

Aims: The aims of this study were to investigate the effects of vitamins A and D in HCT-116 Crl:NU(NCr)-Foxn1nu mouse xenographs. Also, to determine potential mechanisms of action using miRNA-seq and correlated these data with results from RNA-seq.

Methods: HCT-116 colon cancer cells were cultured and used for the xenograph study. Crl:NU(NCr)-Male Foxn1nu mice were injected subcutaneously with HCT-116-cells (1 X 10^6 in 100 µl 50% Matrigel and Sterile PBS), and after 7 days, were treated with vitamin A and D in feed for 21 days. The mice were imaged on day 28, sacrificed and the tumors were excised and measured. RNA was isolated from the HCT-116 cells and tumors, and RNA-seq and miRNA-seq were performed.

Results: There was a concentration-dependent reduction in the HCT-116 colon cancer cell viability after treatment with vitamin A and D combinations. In Crl:NU(NCr)-Foxn1nu mice injected with HCT-116 colon tumor cells, treatment with vitamin A (25,000 IU) and vitamin D (4,000 IU) or vitamin A (35,000 IU) and vitamin D (5,000 IU) for 21 days significantly reduced tumor growth by ~38% and ~58%, respectively ($p < 0.001$). In the HCT-116 cells and excised tumors, treatment upregulated the expression of Bim, Bax, p53, and PTEN, and downregulated AXIN2, ID2 and DDX20 mRNAs, all well-known pro-apoptotic proteins, tumor suppressors, and molecules involved in the epithelial-mesenchymal transition. Ingenuity Pathway Analysis of miRNA-seq paired with RNA-seq showed correlations between miRNAs expression and expression of these genes. For example, miRNA-mRNA correlation pairing showed that treatment downregulated miR-30c-3p and miR-125b-3p which was associated with upregulated TP53. Upregulation of the tumor suppressor PTEN was associated with the downregulation of eleven miRNAs, including oncogenic miR17 and miR21.

Conclusion: The results suggest that the combinations of vitamins A and D reduced the HCT-116 tumor burden in mice and altered the expression of miRNAs directly associated with genes in the apoptosis, tumor suppression, and epithelial-mesenchymal transition pathways. The data supports the hypothesis that vitamin A and D combinations impact multiple cancer signaling pathways and thus may be more effective in the treatment and prevention of cancer, as well as reducing cancer metastasis.

Keywords: apoptosis, cholcalciferol, colon cancer, DDX20, epithelial-mesenchymal transition, ergocalciferol, p53, RNA-seq, miRNA-seq, PTEN, synergism, transcriptome

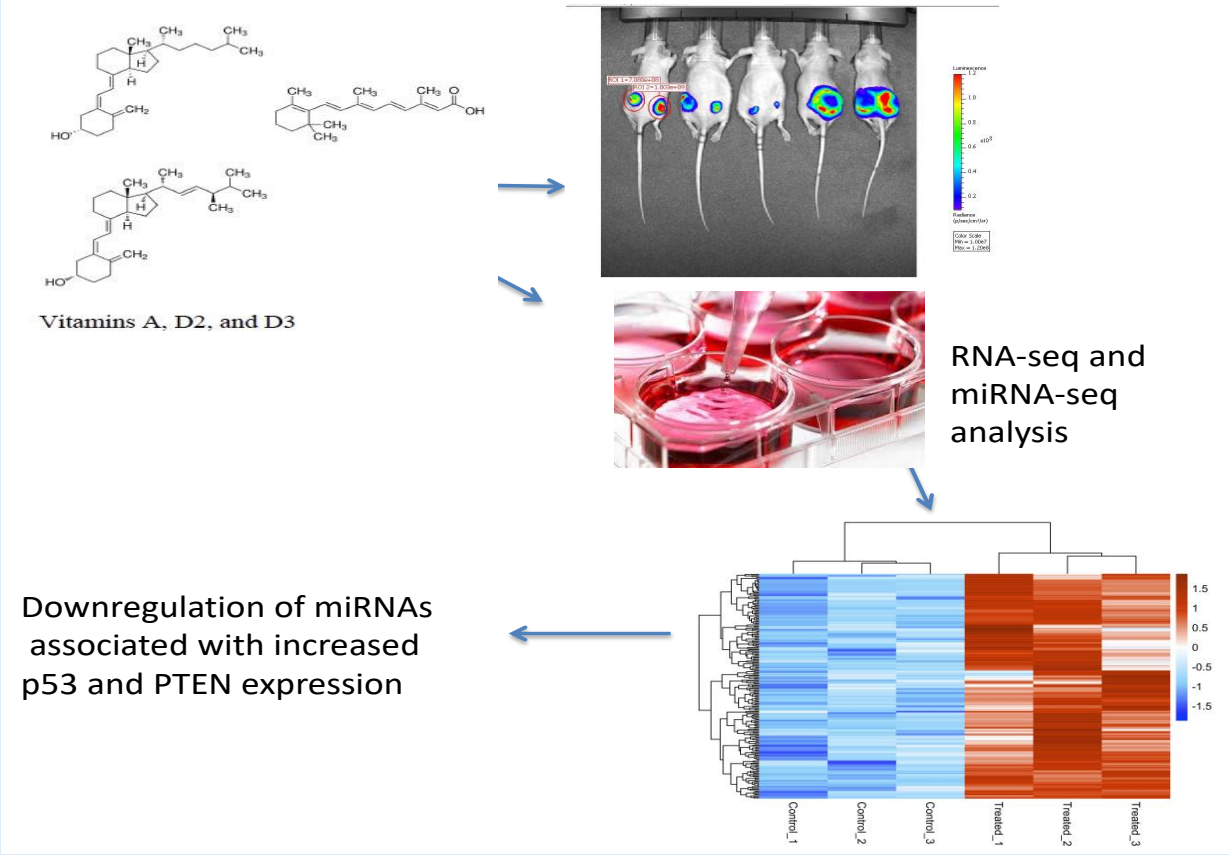

INTRODUCTION

Colorectal carcinoma (CRC) continues to be one of the primary causes of cancer deaths worldwide [1-3]. Numerous factors increase CRC risk, including genetic and racial differences, environment, diet, and lifestyle. These factors include hereditary components and predisposition to polyp formation, as well as alcoholism, high fat diet, large bowel inflammatory disease, obesity, smoking, and stressors [1–3]. Symptoms of CRC usually do not appear until late in the disease progression, thus annual screening is essential for long-term survival. Vitamins A and D have significant anticancer activities as have been shown in clinical trials, as well as in ecological, epidemiological, geographical, observational, and mechanistic studies [4-10]. Vitamin D deficiency significantly increases the risk of breast, colon, gastric, prostate, and other cancers, and patients with low vitamin D levels have a poorer prognosis in gastric cancers [11]. Conversely, patients with elevated serum vitamin D3 (Cholecalciferol, animal based) levels and colorectal cancer had a better prognosis, as well as reduced recurrence, metastasis, and mortality [12-18]. Similar data are available for ergocalciferol (vitamin D2, plant based), as well as vitamin A and all trans retinoic acid (ATRA) show that these nutrients inhibit the growth of breast, colorectal, and gastric cancers, as well as leukemia [19-28]. However, there are few studies that have investigated the effects of these vitamins in combination for the prevention and treatment of cancers.

Over the past few years, our group has been investigating the synergistic effects of the fat-soluble vitamins A and D combinations, as they are normally present together in many functional food products [27-29]. We have previously reported that vitamin A, D2 and D3 combinations induced apoptosis in HCT-116 and SW 480 colon cancer cells by increasing caspase 3/7 and 8 expression and activities, the expression of Bax and BIM (BcL2L11) and other tumor suppressors, including p53 [27-28]. Furthermore, RNA-seq analysis demonstrated that vitamin A and D combinations significantly altered the expression of numerous genes in the HCT-116 colon cancer cells including the expression of mRNAs involved in numerous canonical pathways associated with apoptosis, autophagy, cellular senescence, the epithelial mesenchymal transition (EMT), and immunity [29].

Along with mRNA, microRNAs (miRNAs) play a critical role in cell growth, differentiation, migration, and miRNAs are known to be dysregulated in cancer [30-33]. MicroRNAs (MiRNAs) are a class of small single-stranded non-coding RNAs that bind to messenger RNAs and alter their expression by post-translational modification [33]. By doing so, miRNAs control gene expression associated with many cellular functions including apoptosis, cell proliferation and differentiation, as well as progression of the cell cycle [30-33]. Up-regulation of miRNAs expression inhibits gene expression, while down-regulation of miRNAs increases mRNA expression. MicroRNAs play a central role in the initiation and progression of colon cancer and have now emerged as novel diagnostic and prognosticative tools for many types of cancer [30-33]. Since miRNAs are dysregulated in colon cancer, investigating the impact of specific treatments on miRNA expression can facilitate an understanding of novel mechanisms of action and potential treatments.

Here, we investigate the impact of vitamins A and D treatments in an HCT-116 xenograph mouse model of colon cancer, and further investigate potential mechanisms of action by transcriptomic profiling of HCT-116 colon cancer cells using mRNA and miRNA sequencing (mRNA-seq; miRNA-seq). Co-expression networks were developed using Ingenuity Pathway analysis to identify the interactions among the mRNA:miRNA pairs. The data showed the alterations in the expression of multiple miRNAs that were directly associated with differential gene expression (DGE) of

tumor suppressors, and molecules associated with apoptosis and the EMT.

MATERIALS AND METHODS

Cell culture and maintenance: The HCT-116 and HCT-116-luc colon cancer cells were obtained from American Type Culture Collection (ATCC) and cultured as we have previously described [27-28]. Briefly, the HCT-116 cells were cultured in McCoy's 5a medium supplemented with 10% FBS and 1% Penicillin/Streptomycin and incubated at 37°C in a humidified atmosphere of 5% CO_2 and 95% air. The cells were harvested when they reached 80% confluence, after the addition of 0.25% trypsin/EDTA, and plated in 96 or 6 well plates for the assays. The HCT-116 cells were treated with ATRA+D2+D3 at the IC_{50} concentration (1μM), then harvested and RNA was isolated as we have previously described [27-28].

HCT-116-luc xenograph mouse model: Xenographs were established using fifteen Crl:NU(NCr)-Foxn1nu male mice (4-6 wks old, ~18-19 gms body weight; 3 arms x 5 mice per arm) obtained from Charles River Laboratories. All mice were housed in cages in a controlled environment in Rm 112 of the BRL (72ºC; 14/10-h light/dark cycle) and housed under barrier pathogen free conditions for 7 days prior to initiation of the study. The animals were fed a purified diet specific for imaging (Purina Test Diet AIN-93G #5800) from Purina Mills Inc., St Louis, MO, and given water ad libitum and cared for as detailed in ACC Protocol number 17-116. Group 1: After 7 days of acclimatization, N = 5 Crl:NU(NCr)-Foxn1nu mice were subcutaneously injected with HCT-116-luc cells (1 X 10^6 in 100 µl 50% Matrigel and Sterile PBS) into the flank under 2% isoflurane anesthesia using a 26G needle and 1 ml syringe, and then on day 8 they were treated with the purified diet (containing PBS only negative control) for 21 days. Group 2: After 7 days of acclimatization, Crl:NU(NCr)-Foxn1nu mice (n = 5) were subcutaneously injected with HCT-116-luc cells (1 X 10^6 in 100 µl 50% Matrigel and Sterile PBS) into the flank under 2% isoflurane anesthesia. On day 8 they were treated with the purified diet containing Vitamin A (retinol) 25,000 IU/Kg and vitamin D3 4,000 IU/Kg body weight for 21 days. Group 3: After 7 days of acclimatization, N = 5 Crl:NU(NCr)-Foxn1nu mice were subcutaneously injected with HCT-116-luc cells (1 X 10^6 in 100 µl 50% Matrigel and Sterile PBS) into the flank under 2% isoflurane anesthesia and on day 8 treated the purified diet containing 35,000 IU Vitamin A (retinol) and vitamin D3 5,000 IU/Kg body weight for 21 days. The doses were based on the human dose equivalent and our preliminary in vitro data [34].

***Imaging and data analysis*:** The mice were palpated (tumor measurement) and imaged once weekly. For the HCT-116-luc cells xenographs, we used fluorescence in vivo imaging of the animals to follow the progression and development of the tumors. Before image collection on day 8, all animals were anesthetized using 2% isoflurane and luciferin (intraperitoneal injection, dose 150 mg/kg body weight), as we have previously described [35]. Image collection was performed using a Xenogen IVIS 200 Series live animal imaging system (Xenogen Corp., Alameda CA) for the detection of the luciferase signal. Photon emitted per second (in photons/second/cm2/steradian) from each ROI (region of interest) was quantified using the Living Image® software. Imaging began on Day 8 after the tumor cell injections and then once weekly. At 21 days after treatment the animals were sacrificed using continuous flow CO_2 from a bottled source and cervical dislocation. Tumors and tissues were resected, weighed, and measured using calipers. The body weight of the mice, as well as food and water ingestion were documented twice a week throughout the study. Tumor volume was measured by digital caliper and calculated using the

formula: L1 x L2 x H 0.5238, where L1 = long diameter L2 = short diameter and Height = height of the tumor. After 21 days of treatment or if the tumor volume reached to ~ 1000 mm^3 animals were sacrificed using CO_2 inhalation. Excised tumors were weighed and frozen at − 80 ºC for later RNA extraction and qPCR. The results were calculated by dividing the mean tumor volume or weight of the treated group to that of vehicle control group.

RNA isolation and quality control: HCT-116 colon cancer cells were cultured at a density of 1.0 – 1.2 x 10^6 cells in 1 ml per well of a 6-well plate and incubated overnight as we have previously described [29]. Total RNA and proteins were extracted using Trizol (ThermoFisher Scientific, Waltham, MA, USA) from cultured cells treated with vehicle solvent (0.01% DMSO) or the IC_{50} concentration of ATRA+D2+D3. RNA isolation from excised tumors was performed using Trizol, and the quality of the RNA (RIN number) was determined using an Agilent 2100 Bioanalyzer (Agilent Tech., Palo Alto, CA). Isolated RNA samples were used to generate parallel mRNA-Seq, miRNA-seq and qPCR data. RNA samples were quantified using NanoDrop™ One Spectrophotometer (Thermo Scientific) and analyzed for integrity using Agilent 4200 TapeStation and RNA Screen Tape (PN: 5067-5576). The relative levels of remaining DNA were checked using dual RNA/DNA measurements in a Qubit fluorometer (Invitrogen). The levels of DNA did not exceed 10%.

mRNA-seq data collection: Briefly, the sequencing libraries for Illumina sequencing were prepared using 250 ng of total RNA per sample exactly as we have previously described [29]. Library preparation was carried using a Universal Plus mRNA-Seq library preparation kit (Tecan/NuGen, 0520-A01), as described in the product manual (NuGen, M01485 v5). Final library purification was performed using Agencourt AMPure XP Beads (Beckman Coulter A63881). The final amplified libraries were measured using a Qubit 1X dsDNA HS Assay Kit (Invitrogen, Q33231). The final library pool concentration was confirmed by qPCR and test sequencing was performed to confirm sequencing efficiencies and to adjust proportions of individual libraries. The library pool was purified using Agencourt AMPure XP Beads (Beckman Coulter A63881) and quantified by qPCR using a KAPA Library Quantification Kit and sequenced on a NovaSeq 6000 S4 flow cell, 2x150 bp, approximately 30 M clusters per sample, at the University of Illinois Roy J. Carver Biotechnology Center High-Throughput Sequencing and Genotyping Unit.

miRNA-seq data collection: Total RNA was isolated from cell samples from HCT-116 colon cancer cells treated with vehicle solvent (Control, DMSO 0.01%) or ATRA+D2+D3 (IC_{50} 1 µM). Total RNA was used for miRNA library construction with the QIAseq miRNA library prep kit for Illumina (Qiagen, 331505). Isolated total RNA quality was measured resulting in RNA Integrity Number (RIN) scores ≥ 9.6-10. Sequencing libraries were prepared using total RNA at 250 nanograms per sample. Library construction included the ligation of mature miRNA to specific 3' and 5' adapters [30, 36]. The ligated miRNAs were then reverse transcribed to cDNA using a reverse transcription (RT) primer with a UMI. cDNA cleanup was performed using a magnetic bead-based method. Following cDNA cleanup, library amplification was performed with a universal forward primer and indexing reverse primers where each sample was assigned a unique custom index. Following a final library cleanup using an Agencourt RNAClean XP Bead assay (Beckman Coulter, PN: A63987), each miRNA library was quantified using Qubit 2.0 Fluorometer (Invitrogen) and pooled in equimolar concentrations. Final sequencing pool was analyzed using Tape Station gel analyzer (Agilent) and re-quantified using the qPCR KAPA Library Quantification Kit (KAPA Biosystems). Sequencing was carried out on NovaSeq6000 SP flow cell, 1x100 nt reads, to achieve approximately 20 M reads per sample.

Bioinformatics Analysis and Database Annotation: Bioinformatic analysis of the mRNA-seq raw data was performed by the University of Illinois at Chicago Core for Research Informatics (UICCRI) exactly as we previously have described [29]. Briefly, quality-control for the mRNA sequencing data was obtained using FastQC and raw reads were aligned to human reference genome hg38 in a splice-aware manner using STAR and BWA MEM as we have described [29]. Analysis of the molecular functions and biological processes of differentially expressed genes (DEGs) detected from RNA-seq was performed using the ENSEMBL database (www.ensembl.org) using FeatureCounts [37-38]. EdgeR was used to compute differential expression statistics on raw expression counts with the exactTest function [39]. P-values were adjusted for multiple testing using the false discovery rate (FDR; q value) with the correction as described by Benjamini and Hochberg [40]. DEGs were categorized into functional clusters based on Gene Ontology (GO) function enrichment analysis using edgeR and DeSeq2 [29].

For miRNA, raw reads were trimmed to remove adapters sequence using cutadapt [41]. Reads with no adapter were discarded. Remaining trimmed reads were reads were aligned to mature known human microRNA database obtained from miRbase using BWA ALN [42]. miRNA expression levels where quantified by counting the number of reads mapped to each miRNA sequence and normalized to counts-per-million units for direct comparison between samples. Differential expression statistics were computed using edgeR [43] on raw expression counts with the exactTest function. P-values were adjusted for multiple testing using the false discovery rate (FDR) correction of Benjamini and Hochberg [40]. Bland plots were performed as described in edgeR [44,45].

Data and Statistical analysis: Data from in vitro assays were analyzed using the GraphPad Prism 9.0 software to determine IC_{50} concentrations. Statistical analysis was performed using the Student *t* test in GraphPad version 9.0 (San Diego, CA). The level of significance between the treatments groups as compared with control was estimated by one-way analysis of variance (ANOVA) followed by Tukey's multiple comparison tests. For in vivo studies, the number of animals was calculated using a power/sample analysis, anticipating differences for the treated versus untreated groups (Instat Statistical software). The proposed sample size of 5 mice per group should be sufficient to detect a 50% reduction in outcomes (tumor size/volume) with a power of 80% using a *t*-test where P was considered statistically significant at ≤ 0.05.

Ingenuity® Pathway Analysis (IPA): Ingenuity Pathway Analysis (IPA) was used to identify the canonical and molecular signaling pathways and gene networks that were correlated with observed changes in the transcription levels, and DEGs were further analyzed according to the predicted protein function using the Ensembl database [29, 46]. Differential gene expression and statistical data were uploaded into the Ingenuity® Pathway Analysis software (Qiagen, USA) and analyzed as we have previously described [29] using a false discovery rate (q value) ≤ 0.05. The results were mapped to IPA's knowledge bases, as well as the significant biological functions, networks and pathways.

Quantitative polymerase chain reaction to validate candidate genes: Quantitative PCR (qPCR) was used to validate the transcriptome levels of fragments per kilobase of transcript per million mapped reads (FPKM) generated by RNA-Seq as we have previously described [29]. Total RNA was reverse transcribed and amplified using a Power SYBR Green RNA-to-CT 1- step kit (Applied Biosystems, Foster City, CA, USA) on a Step One Plus Real Time PCR System (Applied Biosystems, Foster City, CA, USA) exactly as we have described [29]. Each reaction (performed in triplicate) contained Power SYBR Green

RT-PCR Mix (2X), 200 nM of each primer, RT Enzyme Mix (125X) and 100 ng RNA. The cycling conditions were as follows: 48°C for 30 min, 95°C for 10 min, followed by 50 cycles of 95°C for 15 sec. and 60°C for 1 min. PCR reaction specificity was confirmed by melt curve analysis at 95°C for 15 sec, 60°C for 15 sec, 95°C for 15 sec. The qRT- PCR assays were conducted in triplicate and $^{\Delta}$Ct values (Ct for GADPH or β-actin - Ct for the test gene) were calculated for each RNA sample. The Student t-test was used to analyze significance between the mean $^{\Delta}$Ct for the control vs. the treated HCT-116 groups, with a threshold significance level $p< 0.05$. The fold change in gene expression was calculated as $^{\Delta\Delta}$Ct ($^{\Delta\Delta}$Ct = $^{\Delta}$Ct of the treatment group - $^{\Delta}$Ct of control group). The qPCR assays were conducted in triplicate and $^{\Delta}$Ct values (Ct for GADPH or β-actin-Ct for the test gene) were calculated for each RNA sample. The specific primers used were (forward (F) and reverse (R) primers, respectively): GADPH: (F) 5'-ACCACAGTCCATGCCATCAC-3' and (R) 5'-TCCACCACCCTGTTGCTGTA-3'; β-actin: (F) 5'TGACGTGGACATCCGCAAAG-3' and (R) 5'-CTGGAAGGTGGACAGCGAGG-3'; ID2 (F)5'-ATGAAAGCCTTCAGTCCCGT-3' and (R) 5'TTCCATCTTGCTCACCTTCTT-3'; PTEN (F) 5'-CCG AAA GGT TTT GCT ACC ATT CT-3' and (R) 5'-AAA ATTA TTT CCT TTC TGA GCA TTC C-3'; p53 (F) 5'-GTCACAGCACATGACGGAGG-3' and (R) 5'TCTTCCAGATGCTCGGGATAC-3'; DDDX20(F) 5'-AGGCATAAAGAAGGCGCTAAC-3' and (R) 5'-GGGTTCTGACTGTACTCGGTAAG-3'; BIM: (F) 5'-ATGTCTGACTCTGACTCTCG-3' and (R) 5'-CCTTGTGGCTCTGTCTGTAG-3'; BAX: (F) 5'-GGCTGTGTTGCTGTGAATC-3' and (R) 5'-GGTATCTGGGAGTAAGGAGGAG-3', using published primers and NIH Primer BLAST [47-50]. GADPH and β-actin were used to control and calibrate cDNA synthesis.

Data sharing and availability: All of the raw datasets for the mRNA-seq and miRNA-seq supporting the conclusions of the work have been deposited and are currently available at the National Center for Biotechnology Information Gene Expression Omnibus repository (GEO), number GSE160109, https://www.ncbi.nlm.nih.gov/geo.

RESULTS

Vitamin A and D combinations reduce the viability of HCT-116 colon cancer cells in culture and the growth of HCT-116 induced xenograph tumors: Vitamin A and D combinations (ATRA+D2+D3) induced apoptosis and reduced proliferation of HCT-116 colon cancer cells (Figure 1A). As compared with ATRA alone, the combination treatment was more effective in reducing cell proliferation. In Crl:NU(NCr)-Foxn1nu mice, colorectal cancer developed after subcutaneous injection of HCT-116 colon cancer cells and after day 7, tumors were apparent, and the animals were administered vitamin A (25K or 35K IU) with Vitamin D (4 or 5K IU) in feed for 21 days. Figure 1B shows that the weight of the mice injected with HCT-116 colon tumor cells and then treated as follows: group 1 (negative control); group 2 (treated with 25,000 IU Vitamin A and 4,000 IU Vitamin D); or group 3 (treated with 35,000 IU Vitamin A and 5,000 IU vitamin D) for 21 days did not significantly differ. In Figure 1C, tumor volume of mice after 21 days of treatment with vitamin A & D 25/4K or 35/5K IU/Kg body weight was significantly reduced in a time-dependent manner. At the end of 21 days, comparison of Crl:NU(NCr)-Foxn1nu mice injected with HCT-116 colon tumor cells, treatment of the animals with 35,000 IU Vitamin A and 5,000 IU vitamin D human dose equivalents reduced tumor growth by ~58% ($p < 0.001$), while the lower dose reduced tumor growth by ~38% $P <0.05$ (Figure 2). Mouse xenographs treated with higher doses of vitamins A and D showed a tumor reduction of 85-90%, however the reduction in tumor burden was not statistically significant due to broad confidence intervals (data not shown).

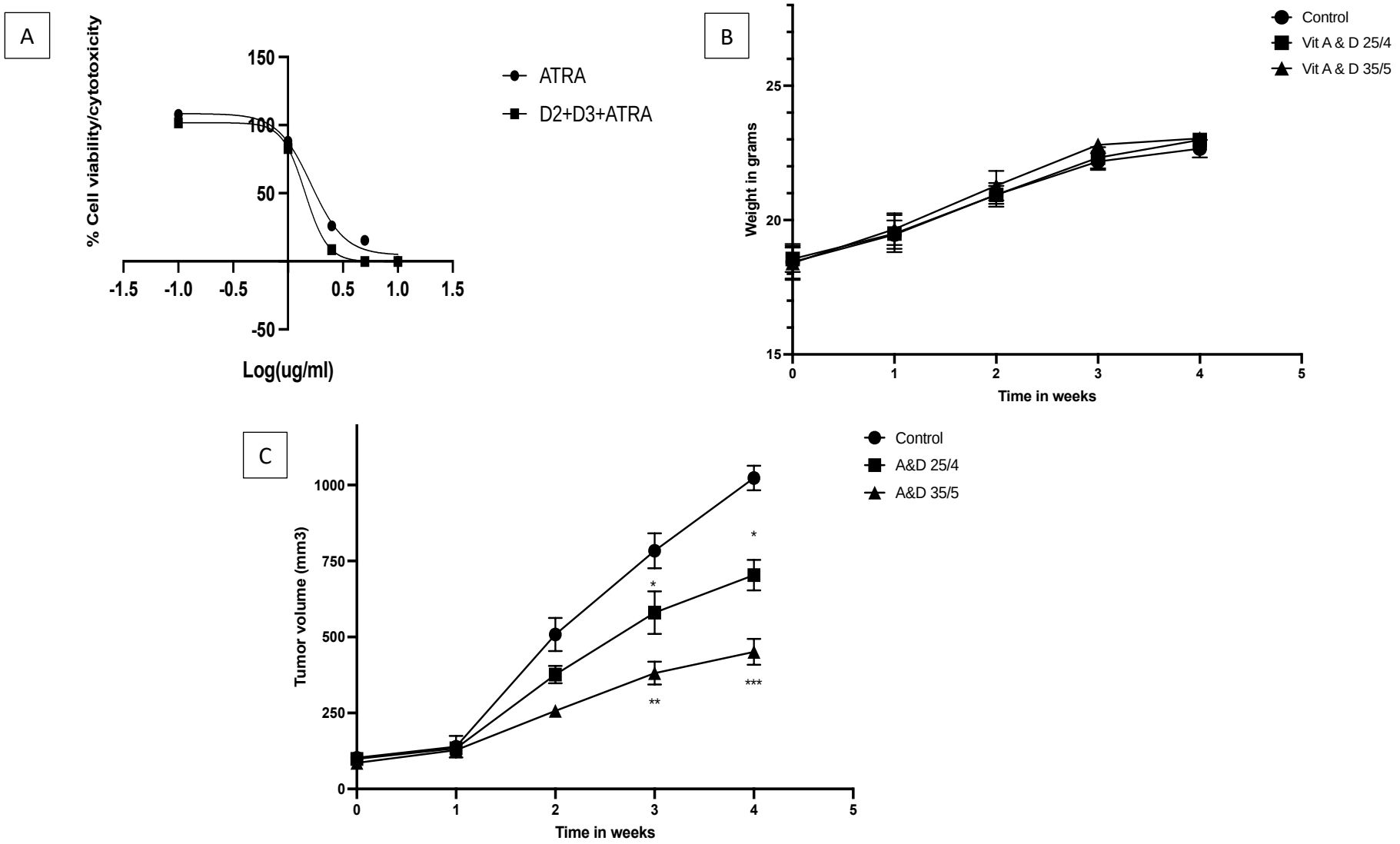

Figure 1A-C. A. Concentration-dependent reduction in HCT-116 colon cancer cell viability after treatment with ATRA or ATRA+D2+D3. **B.** Weight of Crl:NU(NCr)-Foxn1nu mice injected with HCT-116 colon tumor cells, Group 1: negative control; group 2: treated with 25,000 IU Vitamin A and 4,000 IU Vitamin D; group 3: treated with 35,000 IU Vitamin A and 5,000 IU vitamin D for 21 days. **C.** Time dependent reduction in tumor volume in Crl:NU(NCr)-Foxn1nu mice injected with HCT-116 colon tumor cells after treatment with vitamin A & D 25/4 or 35/5 IU/Kg body weight. The means are plotted with SD.

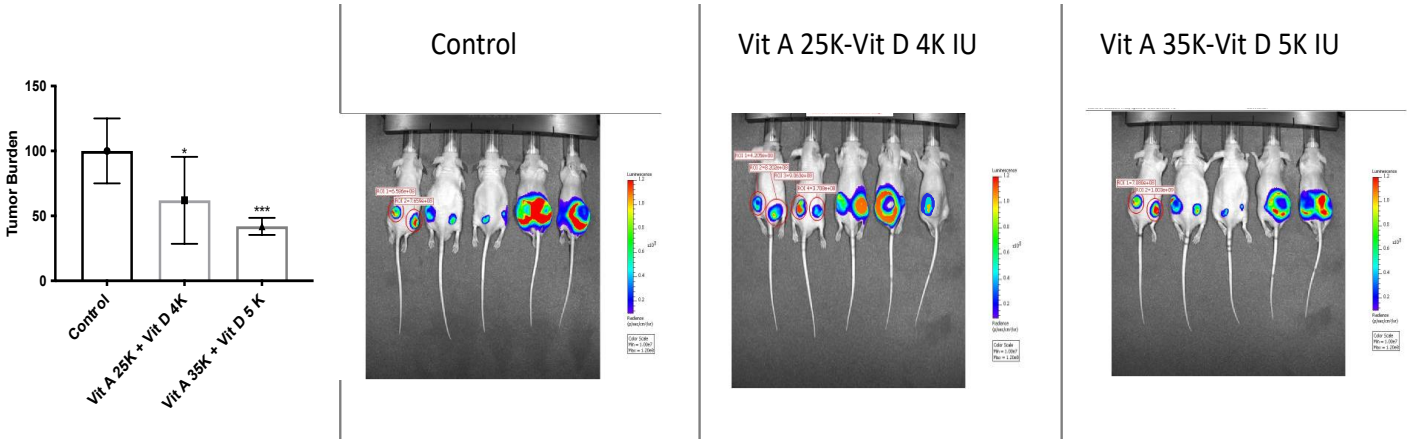

Figure 2. Comparison of Crl:NU(NCr)-Foxn1nu mice injected with HCT-116-luc colon cancer cells. Group 1: Negative control (vehicle solvent); group 2 treated with 25,000IU Vitamin A (retinol) and 4,000 IU Vitamin D for 21 days; group 3 was treated with 35,000 IU and 5,000 IU vitamin D human dose equivalents reduced tumor burden by ~58% ($p < 0.001$), while the lower dose reduced tumor burden by ~38% ($p< 0.05$). Fluorescence was quantified using the Living Image® software and statistics were performed using one-way ANOVA in GraphPad 9.0. * $p<0.05$; ***$p<0.001$.

To understand the mechanisms and signaling pathways by which vitamin A and D combinations impact colon cancer cells, we had previously reported that transcriptomic analysis showed that treatment of HCT-116 cells with vitamins A and D altered the expression of genes in canonical pathways associated with apoptosis, autophagy, cell senescence, EMT and immunity [29]. In this work, we further were interested correlating these data from RNA-seq with the effects of vitamin A and D combinations on miRNA expression in HCT-116 cells using miRNA-seq.

MiRNA profiles of treated versus control HCT-116 colon cancer cells: Principal component analysis (PCA) was prepared from generated miRNA-seq data to assess the observed differences between the control (DMSO 0.01%) and treated (ATRA+D2+D3) HCT-116 cells. Figure 3A shows a distinct difference between the miRNA expression of control versus treated cells in that the treatment group was distantly clustered from the controls in the same PCA plot. These data show distinct differences in the miRNA expression patterns between the control and treatment groups. MiRNA-seq analysis of 2657 potential miRNAs showed that the expression of 818 were significantly altered, with 329 upregulated and 489 down regulated in treated versus control cells (FDR $\leq$ 0.05; Figure 3B MA scatter plot). Statistical analyses were performed with a modified t-test where the p value was further corrected by the Benjamini-Hochberg algorithm [39]. The MA plot (Bland-Altman) was calculated using edgeR [40-41].

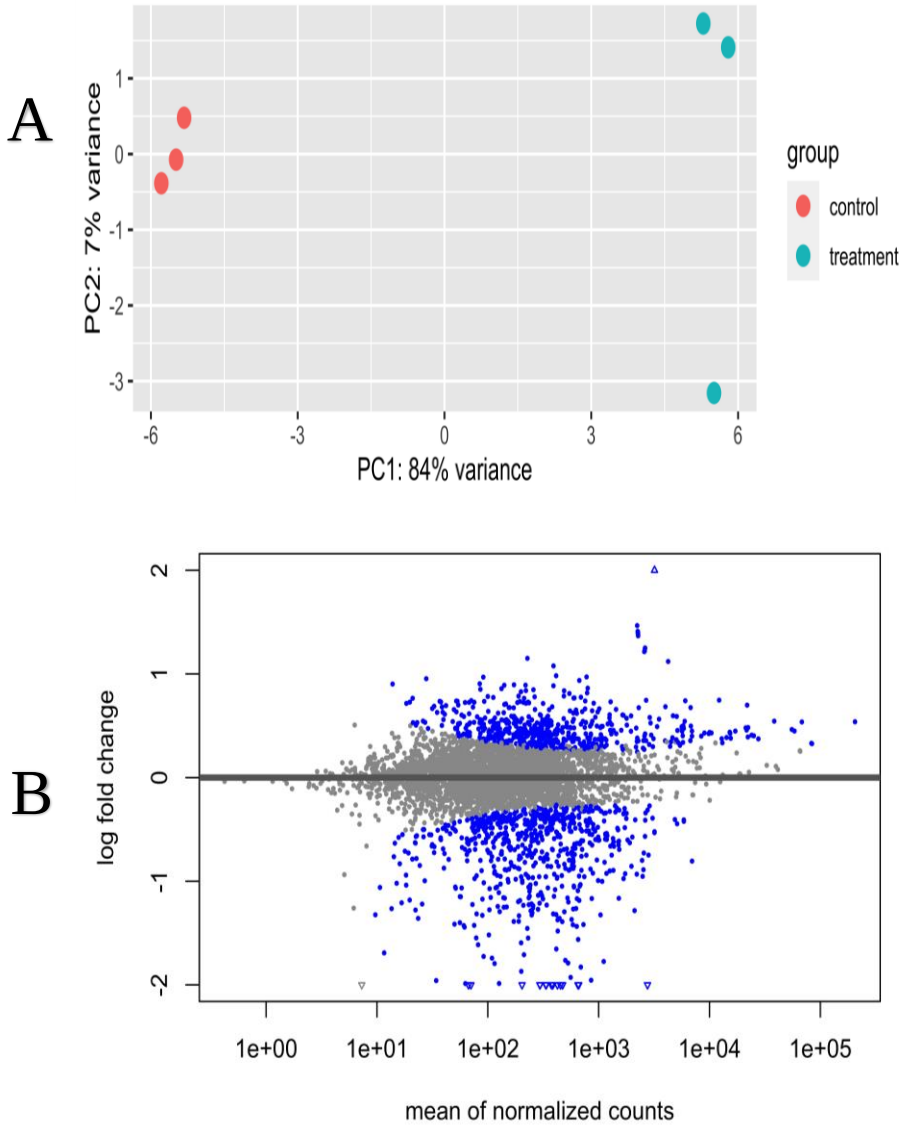

Figure 3A and B. Analyses of the DEGs from miRNA-seq data generated from HCT-116 control cells (DMSO 0.01%) and compared with treated HCT-116 cells (1.0 μg/ml of ATRA+D2+D3). (A) Principal component analysis (PCA) of the six miRNA-seq datasets from HCT-116 colon cancer cells. Control (red dots; DMSO 0.01%) samples; treated samples (blue dots) treated with ATRA+D2+D3. (B) An MA scatter plot shows the relationship between the magnitude of gene expression change (Log fold change, y axis) and the mean of normalized counts. FDR, false-discovery rate. Significantly up and down differentially expressed miRNAs are highlighted in blue, respectively. The expression difference is considered significant at a q value of ≤0.05 (FDR).

Top differentially expressed miRNAs in treated HCT-116 cells: Figure 4 depicts a heatmap for the top 100 differentially expressed miRNAs identified from HCT-116 colon cancer cells treated with ATRA+D2+D3 as compared with control HCT-116 cells (0.01% DMSO), using a false discovery rate (FDR, q ≤0.01) and FC of ≤-1 or ≥ 1. The results showed that 818 miRNAs were differentially expressed, and different gene expression patterns were observed between control and treated HCT-116 cells showing data. The top 20 down-regulated miRNAs in HCT-116 cells treated with vitamins A and D are shown in Table 1, and the top 20 down-regulated

miRNAs are shown in Table 2. Interestingly, miR-494 was the most significantly down-regulated (`-9x) miRNA in treated cells. Using Ingenuity® Pathway Analysis (IPA), the most significant diseases and disorders, as well as molecular and cellular functions associated with miRNA-seq analysis in treated HCT-116 colon cancer cells were determined using an FC of > 1 or -1, and a FDR of < 0.05. Interestingly, the most common disease associated with the changes in miRNA expression was cancer (Table 3). In our previous work, analysis of mRNA-seq from treated HCT-116 cells showed that apoptosis signaling and regulation of the EMT were two of the most important canonical pathways impacted. For example, in the EMT alone, 44 of the 192 genes in the pathway were differentially expressed (Table 4). Here, we further report that treatment of the cells altered gene expression of numerous tumor suppressors and transcription factors namely, p53, PTEN, DDX20, NOTCH1, AXIN2 and ID2, that also play a significant role in the EMT (Figures 5-7). These genes were validated by qPCR in cultured treated HCT-116 cells and excised tumors (Figure 8).

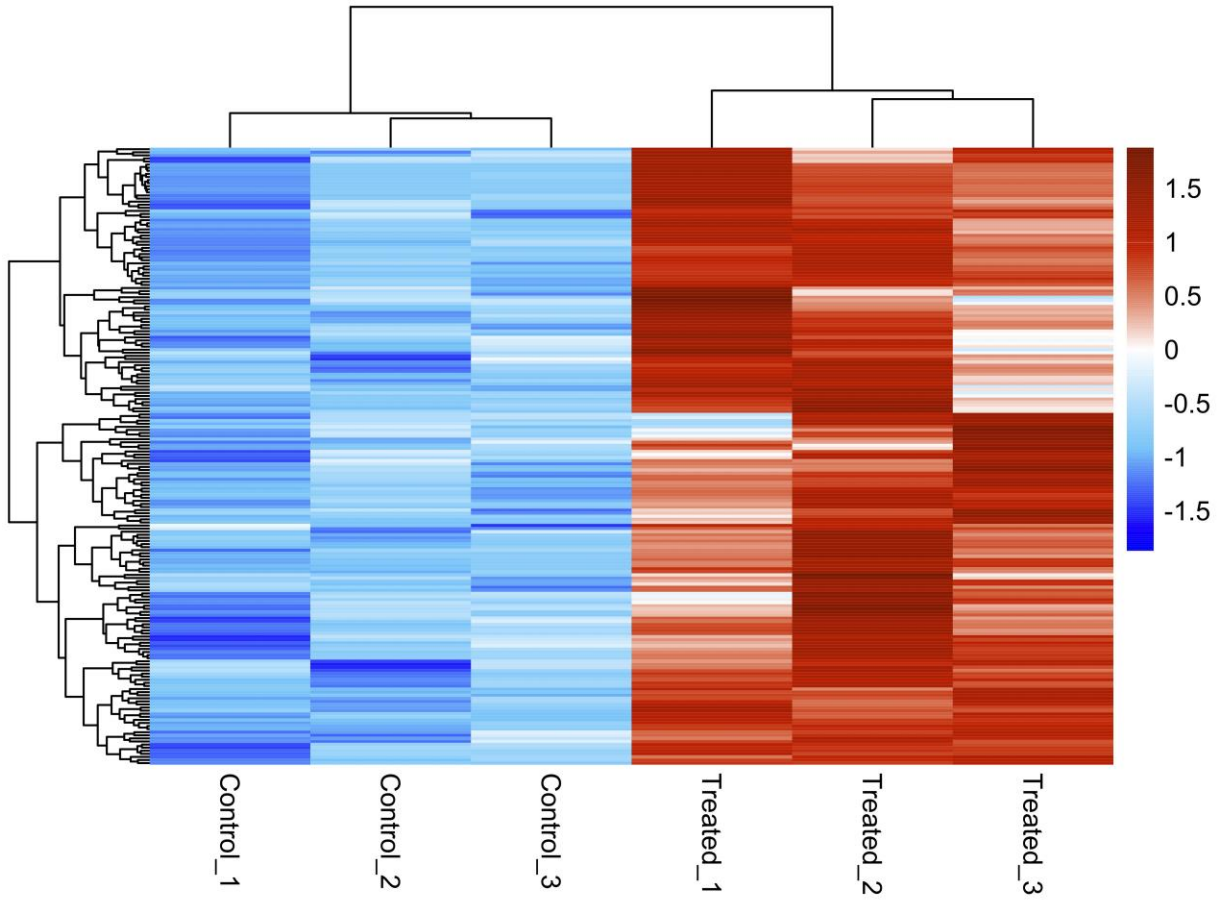

Figure 4. Heatmap depicting the top 100 differentially expressed MiRNAs with gene ontology across data sets. Each column represents the value for one replicate of the experiment, three for control HCT-116 cells, and three for HCT-116 cells treated with 1 μg/ml (IC_{50}) of ATRA+D2+D3 for 4 hours. The colors represent Z-scored Log_2 CPM. To determine the biological functions of the differentially expressed miRNAs, an enrichment analysis of gene ontology is also presented to display the functional distribution.

Table 1. Top 20 down-regulated MiRNAs in HCT-116 colon cancer cells treated with vitamins A and D. Interestingly, MiR-494, a master epigenetic regulator of invasion suppressor miRNAs was the most down-regulated miRNA.

Sequence	ID	Name	FC	Log CPM	P value	Q value
hsa-miR-494-3p	MIMAT0002816	miR-494-3p	-8.71	10.86	6.67E-124	1.77E-120
hsa-miR-4283	MIMAT0016914	miR-4283	-6.61	6.99	2.44E-43	8.10E-41
hsa-miR-662	MIMAT0003325	miR-662	-5.44	8.44	5.36E-55	3.56E-52
hsa-miR-4438	MIMAT0018956	miR-4438	-5.20	8.48	9.44E-51	4.18E-48
hsa-miR-6827-5p	MIMAT0027554	miR-6827-5p	-4.51	9.11	3.68E-56	4.88E-53
hsa-miR-520g-5p	MIMAT0026611	miR-520g-5p	-4.51	10.57	3.44E-52	1.83E-49
hsa-miR-8075	MIMAT0031002	miR-8075	-4.68	10.37	5.79E-45	2.20E-42
hsa-miR-6764-3p	MIMAT0027429	miR-6764-3p	-4.66	10.00	2.79E-55	2.47E-52
hsa-miR-509-3p	MIMAT0002881	miR-509-3p	-4.50	7.90	8.10E-38	1.96E-35
hsa-miR-4473	MIMAT0019000	miR-4473	-4.36	8.22	6.31E-42	1.86E-39
hsa-miR-3926	MIMAT0018201	miR-3926	-4.32	5.61	1.14E-12	3.77E-11
hsa-miR-6833-3p	MIMAT0027567	miR-6833-3p	-4.18	10.19	4.73E-41	1.26E-38
hsa-miR-4264	MIMAT0016899	miR-4264	-4.06	6.47	5.16E-16	2.59E-14
hsa-miR-3649	MIMAT0018069	miR-3649	-4.02	7.35	2.90E-27	3.50E-25
hsa-miR-526b-5p	MIMAT0002835	miR-526b-5p	-4.02	8.55	6.30E-37	1.40E-34
hsa-miR-30e-5p	MIMAT0000692	miR-30e-5p	-3.39	7.76	4.73E-27	5.46E-25
hsa-miR-199b-3p	MIMAT0004563	miR-199b-3p	-3.85	7.01	6.65E-22	6.09E-20
hsa-miR-211-3p	MIMAT0022694	miR-211-3p	-3.81	6.97	2.35E-20	1.73E-18
hsa-miR-324-5p	MIMAT0000761	miR-324-5p	-3.81	7.75	1.21E-26	1.33E-24
hsa-miR-367-3p	MIMAT0000719	miR-367-3p	-3.67	7.42	7.89E-22	6.98E-20

Table 2. Top 20 up-regulated MiRNAs in HCT-116 colon cancer cells treated with vitamins A and D.

Sequence	ID	Name	FC	Log CPM	P value	Q value
hsa-miR-379-5p	MIMAT0000733	miR-379-5p	3.99	6.39564962	5.65E-04	3.18E-03
hsa-miR-3197	MIMAT0015082	miR-3197	3.21	8.53021145	2.03E-21	1.63E-19
hsa-miR-675-3p	MIMAT0006790	miR-675-3p	3.21	8.54822106	2.69E-16	1.38E-14
hsa-miR-525-5p	MIMAT0002838	miR-525-5p	2.67	4.89893212	2.57E-04	1.66E-03
hsa-let-7c-5p	MIMAT0000064	let-7c-5p	2.66	9.56132221	1.04E-13	4.11E-12
hsa-miR-877-5p	MIMAT0004949	miR-877-5p	2.66	7.16692347	5.84E-10	1.30E-08
hsa-miR-6774-5p	MIMAT0027448	miR-6774-5p	2.51	8.90424927	8.19E-15	3.75E-13
hsa-miR-8078	MIMAT0031005	miR-8078	2.36	8.53445444	5.20E-11	1.37E-09
hsa-miR-769-5p	MIMAT0003886	miR-769-5p	2.22	8.63971407	1.42E-06	1.70E-05
hsa-miR-6077	MIMAT0023702	miR-6077	2.14	5.97247836	3.93E-04	2.39E-03
hsa-miR-320b	MIMAT0005792	miR-320b	2.14	12.1560848	1.01E-07	1.59E-06
hsa-miR-1265	MIMAT0005918	miR-1265	2.14	8.58494423	1.89E-11	5.34E-10
hsa-miR-1252-3p	MIMAT0026744	miR-1252-3p	2.12	8.56467914	2.65E-12	8.09E-11
hsa-miR-10395-5p	MIMAT0041621	miR-10395-5p	2.02	5.82407105	1.19E-04	8.59E-04
hsa-miR-1260b	MIMAT0015041	miR-1260b	2.01	9.73403174	1.38E-10	3.48E-09
hsa-miR-583	MIMAT0003248	miR-583	2.01	6.42169381	2.35E-03	0.01046484
hsa-miR-4418	MIMAT0018930	miR-4418	2.01	6.05601011	4.33E-03	0.01765906
hsa-miR-3182	MIMAT0015062	miR-3182	1.89	9.51757682	3.25E-11	8.71E-10
hsa-miR-4269	MIMAT0016897	miR-4269	1.88	7.97790089	2.19E-08	3.99E-07
hsa-miR-875-5p	MIMAT0004922	miR-875-5p	1.88	9.90133171	4.23E-10	1.00E-08

Top Diseases and Bio Functions

Diseases and Disorders

Name	p-value range	# Molecules
Cancer	1.60E-05 - 6.06E-117	2538
Organismal Injury and Abnormalities	1.60E-05 - 6.06E-117	2551
Gastrointestinal Disease	1.60E-05 - 9.46E-73	2232
Endocrine System Disorders	1.30E-05 - 1.22E-71	2134
Dermatological Diseases and Conditions	1.20E-34 - 1.85E-39	1485

1 2 3 4 5 6 7 8 9 >

Molecular and Cellular Functions

Name	p-value range	# Molecules
Gene Expression	1.29E-07 - 6.70E-22	647
Cell Death and Survival	1.00E-05 - 1.15E-17	852
Cellular Movement	3.96E-07 - 3.92E-15	648
Cellular Development	1.54E-05 - 7.03E-14	904
Cellular Growth and Proliferation	1.54E-05 - 7.03E-14	840

Table 3. Using Ingenuity® Pathway Analysis (IPA), the five most significant diseases and disorders, as well as molecular and cellular functions associated with miRNA-seq analysis in HCT-116 cells treated with ATRA+D2+D3 are presented. Alterations in differential miRNA expression were filtered by fold change of ≥ 1 or <-1 and a false discovery rate (FDR) of ≤ 0.05, were used to identify and construct functional networks. Data analysis was mapped to IPA knowledge bases, and their relevant biological functions, diseases and networks.

Vitamin A and D regulate the expression of miRNAs correlated with expression of mRNAs of pro-apoptotic proteins and tumor suppressors in HCT-116 cancer cells: Differential expression of miRNAs (data from miRNA seq) was correlated with DGE from mRNA expression (data from RNA seq) using Ingenuity® Pathway Analysis (IPA). Using the MiRNA pairing and target analysis functions of IPA we were able to pair miRNA expression with mRNA expression. MiRNA-seq showed that HCT-116 cells treated with vitamin A and D altered the expression of many miRNAs that play a role in the regulation of tumor suppressor genes including p53, with miR30c and miR125b being down regulated resulting in the upregulation of p53 (Figure 5). In addition, network analysis of the mRNA-seq and miRNA-seq in IPA showed a correlation between alterations in the expression miRNAs and these specific mRNAs. Upregulation of Bcl2L11 (BIM) was associated with down-regulation of miRNAs, miR19b-3p, miR92a-3p, and miR17-5p. Upregulation of PTEN was associated with downregulation of miR17-5p, miR19b-3p, miR21-5p, miR23a-3p, miR29b-3p, miR92a-3p, miR205-5p, miR200b-3p, miR214-3p, miR494-3p, and miR532-3p (Figure 5).

Table 4. A list of differential expressed genes in the epithelial-mesenchymal transition canonical pathway in cultured HCT-116 cells treated with 1µg/ml of ATRA+D2+D3. Forty-four of the 192 genes in this pathway were differentially expressed after treatment, however only those genes with a false discovery rate FDR < 0.02 were presented in this Table.

Symbol	Entrez Gene Name	Ensembl	FC	Q value
APH1B	aph-1 homolog B, gamma-secretase subunit	ENSG00000138613	1.2	0
AXIN2	axin-like protein (Axil) or axis inhibition protein 2	ENSG00000168646	-7.1	0
DVL1	dishevelled segment polarity protein 1	ENSG00000107404	-1.3	0
EGFR	epidermal growth factor receptor	ENSG00000146648	-1.3	0
EGR1	early growth response 1	ENSG00000120738	2.55	0
ESRP2	epithelial splicing regulatory protein 2	ENSG00000103067	-1.8	0
ETS1	ETS proto-oncogene 1, transcription factor	ENSG00000134954	-1.1	0
FGF1	fibroblast growth factor 1	ENSG00000113578	-4.85	0
FGF9	fibroblast growth factor 9	ENSG00000102678	-4	0
FGF11	fibroblast growth factor 11	ENSG00000161958	2.1	0
FGF18	fibroblast growth factor 18	ENSG00000156427	-4.1	0
FGF19	fibroblast growth factor 19	ENSG00000162344	2	0
FGFR3	fibroblast growth factor receptor 3	ENSG00000068078	-2	0
FOXC2	forkhead box C2	ENSG00000176692	1.6	0.02
FZD2	frizzled class receptor 2	ENSG00000180340	1.3	0
FZD7	frizzled class receptor 7	ENSG00000155760	1.68	0
HMGA2	high mobility group AT-hook 2	ENSG00000149948	-2	0
HRAS	HRas proto-oncogene, GTPase	ENSG00000174775	-1.1	0
ID2	inhibitor of DNA binding 2	ENSG00000115738	-5.16	0
JAG2	jagged canonical Notch ligand 2	ENSG00000184916	-2.88	0
JAK3	Janus kinase 3	ENSG00000105639	1.3	0
MAP2K4	mitogen-activated protein kinase kinase 4	ENSG00000065559	-1.4	0
MAP2K7	mitogen-activated protein kinase kinase 7	ENSG00000076984	-1.45	0
NFKB1	nuclear factor kappa B subunit 1	ENSG00000109320	-1.4	0
NOTCH1	notch receptor 1	ENSG00000148400	-1.44	0
NOTCH4	notch receptor 4	ENSG00000204301	2.24	0
PARD6B	par-6 family cell polarity regulator beta	ENSG00000124171	1.01	0
PARD6G	par-6 family cell polarity regulator gamma	ENSG00000178184	-1.4	0
PIK3R3	phosphoinositide-3-kinase regulatory subunit 3	ENSG00000117461	1.1	0.02
PYGO1	pygopus family PHD finger 1	ENSG00000171016	2.4	0.02
RAP2B	RAP2B, member of RAS oncogene family	ENSG00000181467	1.4	0
RASD1	ras related dexamethasone induced 1	ENSG00000108551	3.4	0
SMAD3	SMAD family member 3	ENSG00000166949	2	0
SMAD7	SMAD family member 7	ENSG00000168646	-5.1	0
SNAI2	snail family transcriptional repressor 2	ENSG00000019549	3.1	0
TCF3	transcription factor 3	ENSG00000071564	-1.2	0
TCF7L2	transcription factor 7 like 2	ENSG00000148737	-1.6	0
TGFB3	transforming growth factor beta 3	ENSG00000119699	1.3	0
WNT2	Wnt family member 2	ENSG00000105989	10.84	0
WNT16	Wnt family member 16	ENSG00000002745	-1.4	0
WNT10B	Wnt family member 10B	ENSG00000169884	-1.4	0
WNT7B	Wnt family member 7B	ENSG00000188064	3.2	0
WNT9A	Wnt family member 9A	ENSG00000143816	1.1	0
ZEB1	zinc finger E-box binding homeobox 1	ENSG00000148516	1.88	0

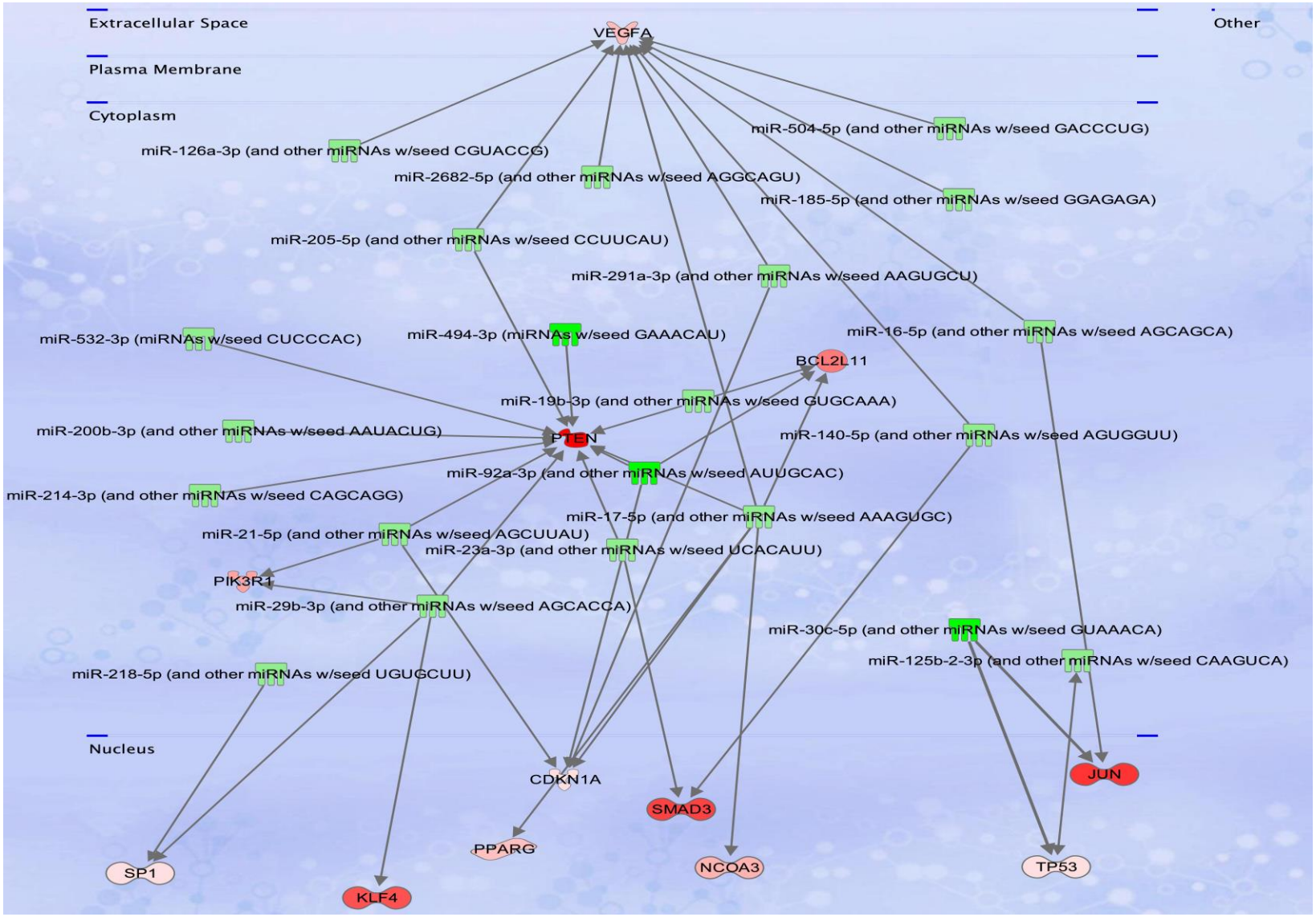

Figure 5. Correlative network analysis of the expression of MiRNAs that were associated with mRNA expression of PTEN, p53, and BIM (BcL2L11) in HCT-116 cells after treatment with ATRA+D2+D3. The genes highlighted in red or pink showed significant upregulation, while the miRNAs highlighted in green or light green showed significant downregulation. Only those DEGs with a false discovery rate FDR < 0.01 are included in this figure. The downregulation of miR-494 was significantly associated with the upregulation of PTEN.

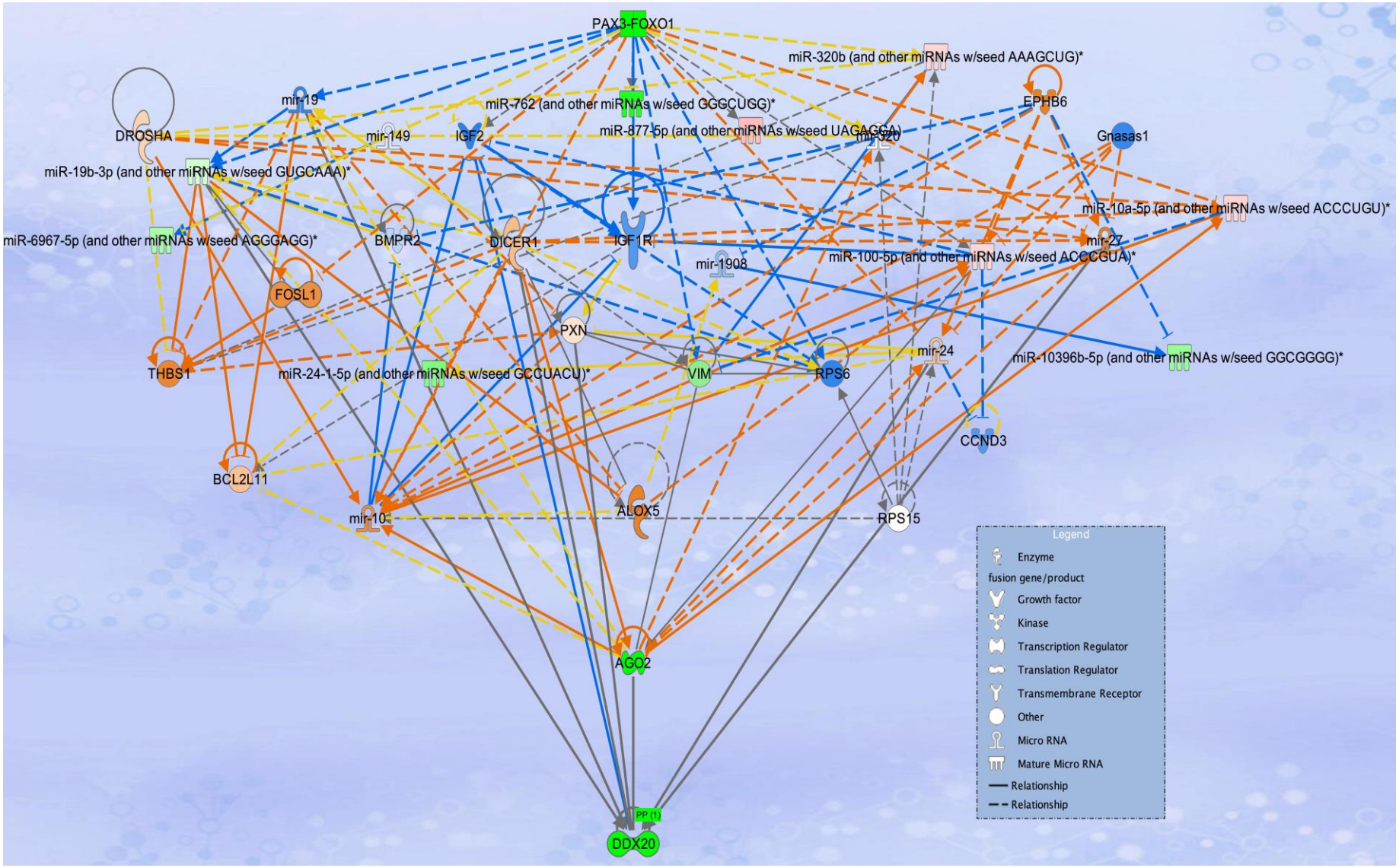

Figure 6. Correlative network analysis of the expression of miRNAs with mRNAs after treatment of HCT-116 cells with ATRA+D2+D3 that impacted apoptosis and epithelial-mesenchymal transition (EMT). Experimental data: genes highlighted in red/pink show significant upregulation and genes highlighted in green/light green show significant downregulation. Downregulation of DDX20 (Gemin3) was associated with miR19 and miR24. Genes in blue show predicted downregulation. Only those genes with a false discovery rate FDR < 0.01 are included in this figure.

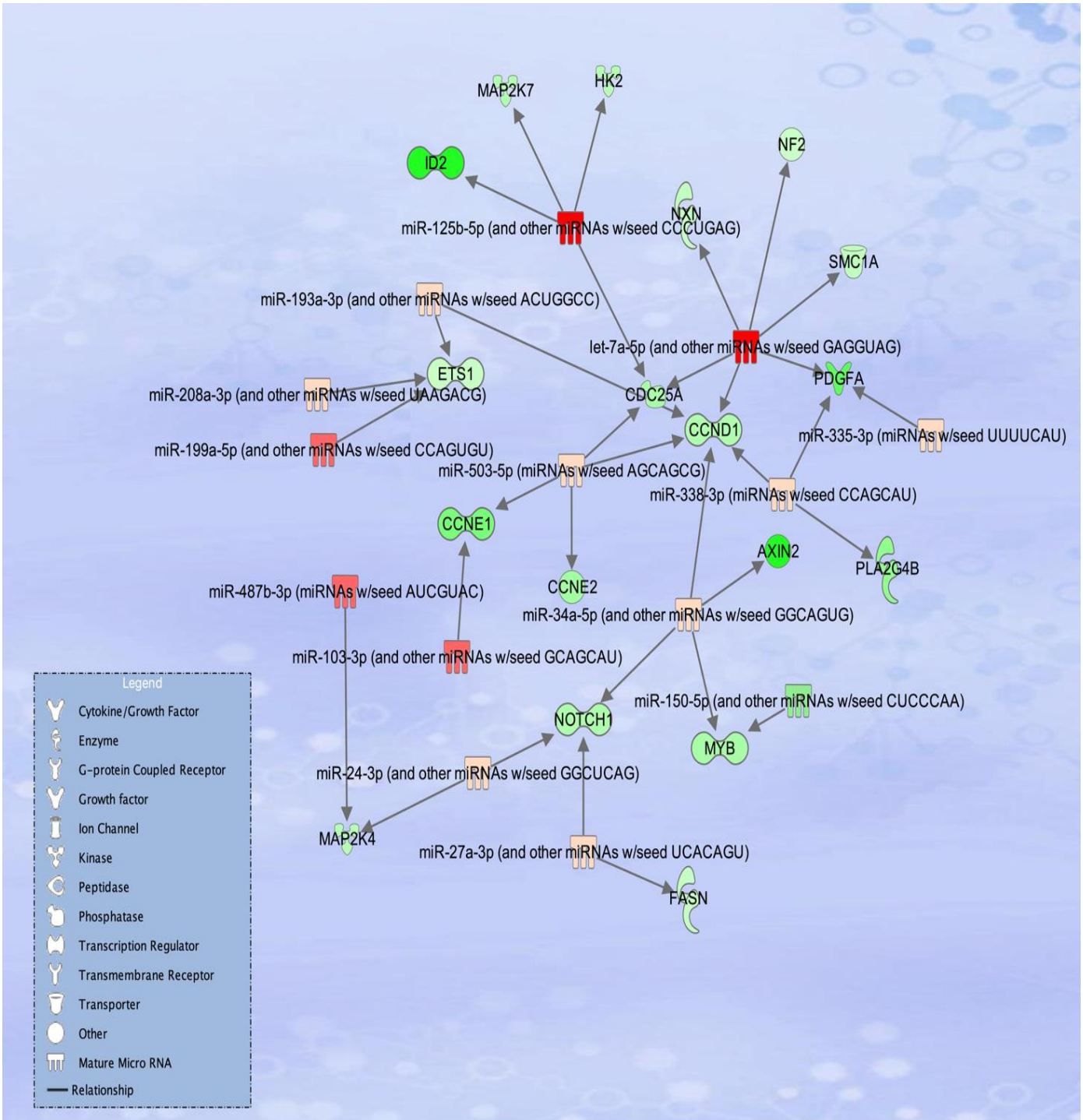

Figure 7: Correlative network analysis of MiRNAs and mRNAs differentially expressed in the cell cycle and EMT pathways in HCT-116 colon cancer cells treated with ATRA+D2+D3. Genes highlighted in red/pink show significant upregulation and genes highlighted in green/light green show significant downregulation. Only those genes with a false discovery rate FDR < 0.01 are shown. Increased expression of miR24-3p and miR27a-3p are associated with downregulation of NOTCH1. Upregulation of miR103-3p, miR503-5p, miR338-3p and let-7a-5p were associated with downregulation in cell cycle genes CCND1, CCNE1and CCNE2. Increased expression of miR34a-5p was associated with downregulation of AXIN2 and miR125b-3p was associated with downregulation of ID2.

Vitamin A and D regulate the expression of miRNAs correlated with expression of mRNAs of DDX20, ID2 and cell cycle proteins in HCT116 colon cancer cells*:* Correlative network analysis of the expression of miRNAs with mRNAs isolated from HCT-116 cells treated with ATRA+D2+D3 showed expression alterations that impacted cell cycle and epithelial-mesenchymal transitions. Downregulation of DDX20 (Gemin3) was associated with miR19 and miR24, with a false discovery rate FDR < 0.01 (Figure 6). Increased expression of miR24-3p and miR27a-3p were associated with downregulation of NOTCH1. Upregulation of miR103-3p, miR503-5p, miR338-3p and let-7a-5p were associated with downregulation in cell cycle genes CCND1, CCNE1and CCNE2 (Figure 7). Increased expression of miR34a-5p was associated with downregulation of AXIN2 and miR125b-3p was associated with downregulation of ID2 (Figure 7).

Validation of DEGs in the apoptosis and EMT canonical pathway by qPCR in vitro and in vivo: The Bcl-2 protein family plays a significant role in apoptosis. To validate the differential expression of genes in both cultured HCT-116 cells and excised tumors from xenographs, qPCR analysis was performed for specific genes in the apoptotic and EMT pathways, as well as tumor suppressors. Total RNA was isolated from HCT-116 colon cancer cells and excised tumors after treatment with vitamins A and D versus control (vehicle solvent) using Trizol. We have previously reported that Bcl proteins are altered in colon cancer cells after treatment with ATRA+D2+D3, and here report that the expression of the pro-apoptotic genes Bax and Bim in xenograph tumor tissues derived from vitamin A and D treated mice was significantly upregulated (Figure 8A). Figure 8A shows an increase in Bax and Bim expression in treated HCT-116 cultured cells and tumors, while ID2 mRNA was reduced in both. In terms of tumor suppressors p53, DDX20 and PTEN, both p53 and PTEN were upregulated, while DDX20 was downregulated in treated cultured cells and tumors, as compared with controls (Figure 8B).

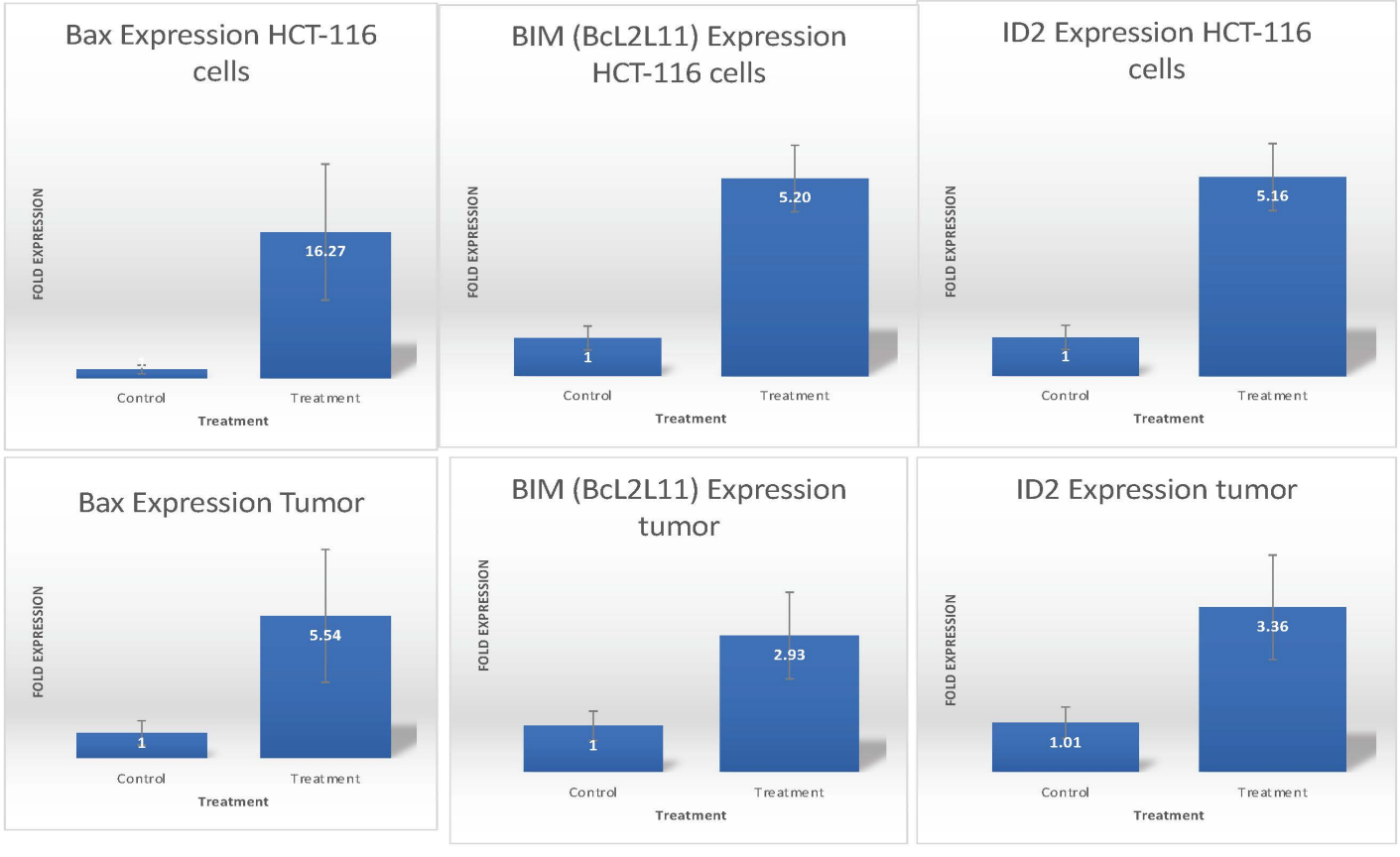

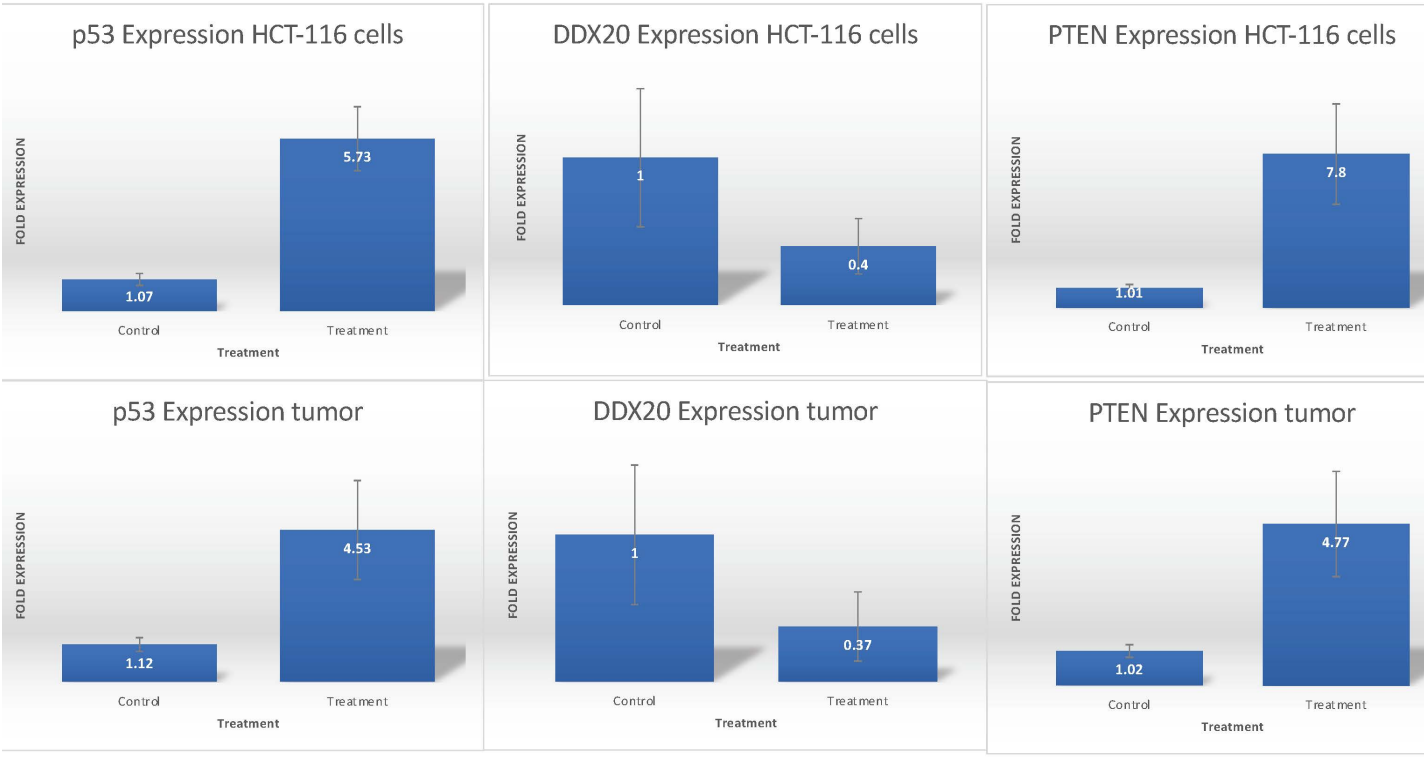

8 B

Figure 8A and B: A. qPCR analysis of relative gene expression of genes apoptotic and EMT pathways in HCT-116 colon cancer cells and excised tumors after treatment with vitamins A and D versus control (vehicle solvent). **A**. Altered gene expression in apoptosis pathways including BAX, BIM and ID2 mRNA in cultured HCT116 cells versus excised tumors. **B**. Altered gene expression of the tumor suppressors p53, DDX20 and PTEN as compared with controls in cultured HCT116 cells versus tumors from Crl:NU(NCr)-Foxn1nu mice injected with HCT-116 colon tumor cells after treatment with vitamin A and D 35/5 IU/Kg body weight.

DISCUSSION

Previously, we have reported that vitamin A and D combinations had synergistic effects in cultured gastric and colon cancer cells, and significantly inhibited the proliferation of HCT-116 colon cancer cells by altering the regulation of multiple signaling pathways including those in cell survival/apoptosis (Bcl-2, Bax, caspase 3/7), and autophagy (mTOR) [29]. In this work, we show that treatment of mouse xenographs with vitamin A and D combinations also significantly reduced the tumor burden by 38- 58% over 21 days as compared with controls. Quantitative PCR analysis showed that the expression pro-apoptotic (Bax, Bim) and tumor suppressor (p53, PTEN) genes were similarly upregulated in both cultured cells and excised tumors. These data correlate with those of Muto et al., [51] who reported that calcitriol induced apoptosis in colorectal adenomas by upregulating pro-apoptotic proteins including Bax, downregulating the anti-apoptotic protein Bcl-2. Furthermore, qPCR analysis showed the expression of the transcription factor ID2 and the helicase DDX20 were significantly downregulated in both HCT-116 cells and xenographs.

Our previous RNA-seq analysis showed that the treatment of cultured HCT-116 cells with ATRA+D2+D3 significantly altered the expression of genes involved in multiple canonical pathways associated with apoptosis, autophagy, cellular senescence, the epithelial mesenchymal transition (EMT), and immunity [29]. IPA data analysis of the RNA-seq data showed that ATRA+D2+D3 treatment of HCT-116 cells increased the expression of Bax, Bim, Noxa, and Puma all involved in

both intrinsic and extrinsic apoptosis [29]. In this work, we report that transcriptomic analysis also showed alterations in the expression of specific transcription factors and tumor suppressors, including PTEN, p53, AXIN2, DDX20 and ID2. In addition, the expression of the E-type cyclins E1 (CcnE1), E2 (CcnE2) that are regulatory subunits of cyclin-dependent kinase 2 and activate the transition of dormant cells into the cell cycle were significantly downregulated, suggesting that vitamins A and D also inhibit the cell cycle. Furthermore, ATRA+D2+D3 treatment of HCT-116 cells significantly altered the expression of numerous genes in the EMT, suggesting potential inhibition of the EMT.

Since it is well known that noncoding RNAs, particularly microRNA (miRNAs), play a central role in regulating many of the signaling pathways that are associated with the development of CRC, we investigated the impact of treatment on miRNA expression in HCT-116 cells using deep sequencing. The miRNA-seq data confirmed that the miRNA expression pattern significantly differed between the control and treatment groups. MiRNA analysis of 2657 potential miRNAs showed that the expression of 818 were significantly altered, with 329 upregulated and 489 down regulated in treated versus control cells (FDR $\leq$ 0.05). MiRNAs are short non-coding RNAs having a length of approximately 20-22 nucleotides and bind to the 3' UTR (untranslated region) of target mRNAs and alter their expression [52-53]. Upregulation of miRNAs in the miRNA-mRNA interaction leads to cleavage of the mRNA and translational inhibition. Thus, miRNAs play an important role in virtually all cellular processes, especially differentiation, proliferation, migration, and apoptosis, and dysregulation of miRNAs plays a significant role in cancer [52]. For example, in our study miR-494, a master epigenetic regulator of invasion suppressor miRNAs was significantly downregulated by ~-9 fold in cells treated with vitamin A and D combinations. MiR-494 is known to be upregulated in human cancers and promotes cancer cell migration and invasion by suppressing the expression of invasion-suppressor miRNAs and inhibiting DNA demethylation of their CpG islands [53]. In knock-down xenograph models, stable miR-494 knockdown reduced the formation of tumors in liver cancer and reduced lung metastasis [53]. Other studies have reported that miRNAs are involved in the antitumor effects of vitamin D, including miR-1278, miR-627 and miR-22, both thought to be important for the anticancer effects of vitamin D in colon cancer [54]. In terms of ATRA, Liu et al. [55] found that treatment of HCT-116 cells with ATRA increased the expression of miR-3666 at concentrations of 20 and 60 µmol that was associated with a reduction in HCT-116 proliferation and invasiveness. Thus, regulating miRNA expression appears to be a promising molecular therapeutic approach for the prevention and treatment of cancers.

One tumor suppressor, p53, plays an important role in apoptosis, cell cycle and metabolism, and can indirectly restrict the conversion of epithelial cells to mesenchymal stem cells [56]. In addition, p53 restricts the EMT process, by inhibiting the activities transcription factors (TFs) associated with the EMT by altering the expression of miRNA's that suppress this process [56]. Loss of p53 function induces the Wnt signaling cascade and promotes a Snail-dependent EMT. In this work, our data show that p53 mRNA is upregulated, and was associated with the downregulation of the expression of miR-125-2-3p. Another tumor suppressor that was significantly upregulated in HCT-116 cells after treatment with vitamin A and D combinations, was phosphatase and tensin homolog (PTEN). PTEN regulates the phosphatidylinositol-3-kinase (PI3K)/AKT signaling cascade that is involved in aspects of apoptosis, cell proliferation, and metabolism [57]. In cancer, PTEN is highly mutated causing a loss of its tumor suppressor activities by altering the P13K/AKT pathway, and

numerous miRNAs are involved in suppressing the expression of PTEN [58-60]. In this work, treatment of HCT-116 cells with ATRA+D2+D3 upregulated the expression of PTEN and downregulated numerous miRNAs including oncogenic miRNA-17, miR-21, and the master epigenetic regulator of invasion suppressor miRNAs, miR-494. MiR-494 is known to target specific tumor suppressor genes, particularly PTEN [53]. Upregulation of miR-17 is reported to suppresses PTEN expression and increases cell motility and invasiveness [58]. Our data show significant downregulation of miR-17, miR-21, miR-200, miR-494 and other miRNAs that increased the expression of PTEN. Tumors with high miR-21 expression are associated with a poorer therapeutic outcome, and novel therapeutics that target miR-21 may have therapeutic benefits in patients with tumors with high expression of miR-21 [31-33]. For example, Schetter et al., [61] identified five miRNAs that were altered in CRC patients and found that miR-21 was overexpressed in 87% of colon cancers specimens, which were associated with a poorer clinical outcomes and cancer prognosis. Furthermore, inhibition of miR-21 inhibited cancer cell growth and tumor growth in xenograft mouse models [62]. Another study has shown that miR-21 targets PTEN further supporting a causal role for altered microRNA expression during tumorigenesis [63].

Interestingly, upregulation of other EMT associated transcription factors inhibits the transcription of miRNAs that function in concert with the p53 to modulate the EMT pathway [64]. Our data also confirmed the downregulation of the DNA-binding protein inhibitor ID-2, a transcription regulator that forms heterodimers with basic helix-loop-helix transcription factors and prevents their binding to DNA, thereby inhibiting their transcriptional activities [65]. The ID proteins are highly expressed in cancer stem cells, and increase their proliferation, while reducing differentiation [65]. ID2 is specifically regulates angiogenesis, apoptosis, cell proliferation and differentiation, as well as neoplastic transformation, and activated ID2 increases cell proliferation and reduces apoptosis. Over expression of ID2 has been reported in colon cancers and has been attributed to the activation of the ID2-promoter due to increased expression and activation of β-catenin [65]. In the EMT, ID proteins are dysregulated, thereby increasing tumor growth, vascularization, invasiveness, metastasis, and stem cell proliferation. In this work, upregulation of miR-125b was correlated with significant downregulation of ID2 expression, while the expression of p53 was significantly upregulated. Paolella et al., [64] have also shown that ID2 expression was downregulated by p53, and p53 acted as repressor of ID2 gene expression by binding a conserved site within its promoter [64]. Thus, out data support these observations.

Also involved in the EMT are the DEAD-box RNA helicases that have several conserved motifs within their helicase core and require adenosine triphosphate (ATP) hydrolysis for RNA chaperoning and RNPase activity [66]. Dysregulation DEAD-box helicases, including DDX20 (also known as Gemin3) are reported to have negative effects on cellular homeostasis, and may result in uncontrolled cell proliferation, survival of damaged cells, as well as increased invasiveness that may cause cancer initiation and progression [66]. In an engineered organotypic colon cancer model containing cell-populated mucosa that mimics CRC progression to submucosal invasive tumors, six genes including DDX20, FXR1, MITF and PAX7, were found to significantly promote submucosal invasion in this model [67]. Mechanistically, DDX20 can specifically bind to the DNA-binding domain of p53 thereby blocking p53-mediated tumor suppressor activities and apoptosis [64, 68]. Our data show that treatment of HCT-116 cells with ATRA+D2+D3 significantly reduced the expression of DDX20 via upregulation of several miRNAs, suggesting that that vitamins A and D may also reduce tumor load by inhibiting DDX20 signaling.

CONCLUSIONS

In this work we have demonstrated that vitamins A and D combinations reduced the growth of HCT-116 colon cancer cells and tumor in mouse xenographs. The results were both concentration and time dependent. In cultured cells and excised tumors, treatment altered the expression of genes associated with the Bcl-2 family of pro-apoptotic proteins, tumor suppressors, and molecules involved in the epithelial-mesenchymal transition. Further investigation of potential mechanisms of action included the analysis of miRNA, and miRNA-seq characterized alterations in the miRNA transcriptome of treated HCT-116 cells. Deep sequencing showed a total of 818 mature miRNA were expressed, of which 329 were upregulated and 489 were downregulated in treated versus control cells. The most downregulated miRNA was miR-494. Analysis of miRNA-mRNA correlation pairing showed that combination vitamin A and D treatments altered the expression of numerous miRNAs that were directly associated with the expression of tumor suppressors and molecules in the apoptosis, cell cycle and EMT pathways supporting our previous work. Thus, our data support the hypothesis that combinations of vitamin A and D are effective in the treatment of HCT-116 induced colon cancer and may be effective in reducing cancer metastasis by impacting multiple miRNAs and signaling pathways.

List of abbreviations: ATRA: all trans-retinoic acid, Bcl-2: B-cell lymphoma 2, Bax: bcl-2-like protein 4, BIM: Bcl-2-like protein 11, CRC: colorectal cancer, D2: ergocalciferol, D3: cholecalciferol, DGE: differential gene expression, DDX20: DEAD-box helicase 20, EMT: epithelial mesenchymal transition, FC: Fold change, FDR: false discovery rate; GADPH: Glyceraldehyde 3-phosphate dehydrogenase, IPA: Ingenuity Pathway Analysis, Noxa: Phorbol-12-myristate-13-acetate-induced protein, PCA: principal component analysis, PUMA: p53 upregulated modulator of apoptosis, PTEN: phosphatase and tensin homolog, qPCR: quantitative polymerase chain reaction

Competing interests: The authors declare that there are no conflicts of interest.

Authors' contributions: GBM, TOL, SP, NAR designed and conducted the research. SP and TOL isolated the RNA and NSL and ZA performed the RNA purification, miRNA-seq and RNA-seq; PNK and MMC performed the Bioinformatics and statistical analyses. GBM, TOL, SP grew, treated and harvested the HCT-116 cells, NL and PNK isolated RNA, analyzed data, GBM performed IPA and imaging analyses, wrote and edited the manuscript.

Acknowledgements and Funding: We would like to express our sincere appreciation for the generous educational sponsorship from the First Analysis Institute of Integrative Studies (GBM); a research grant from the Regenstein Foundation (GBM); a Postdoctoral fellowship award from the Schlumberger Foundation (TOL/GBM); and a Raman Post-Doctoral Fellowship by the University Grants Commission, Govt. of India to (NAR/GBM). PK and MMC were supported in part by University of Illinois at Chicago (UIC) Center for Clinical and Translational Science (CCTS) through Grant UL1TR002003. We would like to express our sincere thanks and appreciation to F. Oliver Nicklin at the First Analysis Institute of Integrative Studies for the theoretical discussions, as well as his assistance with hypothesis generation and the direction of the work. The contents are solely the responsibility of the authors and do not necessarily represent the official views of the funding agencies.

REFERENCES

1. Bray F, Ferlay J, Soerjomataram I, Siegel RL, Torre LA, Jemal A. Global cancer statistics 2018: GLOBOCAN estimates of incidence and mortality worldwide for 36 cancers in 185 countries. CA Cancer J Clin. 2018; 68: 394-424. DOI: https://doi.org/10.3322/caac.21492 Epub 2018 Sep 12.
2. Dekker E, Tanis J, Vleugels J, Kasi P, Wallace M. Colorectal cancer. Lancet 2019; 394:1467-1480. DOI: https://doi.org/10.1016/S0140-6736(19)32319-0
3. Arnold M, Sierra MS, Laversanne M, Soerjomataram I, Jemal A, Bray F. Global patterns and trends in colorectal cancer incidence and mortality. Gut. 2017; 66: 683-691. DOI: https://doi.org/10.1136/gutjnl-2015-310912
4. Garland CF, Garland FC. Do sunlight and vitamin D reduce the likelihood of colon cancer? Int J Epidemiol 1980; 9:227-231. DOI: https://doi.org/10.1093/ije/9.3.227
5. Garland CF, Comstock GW, Garland FC, Helsing KJ, Shaw EK, Gorham ED. Serum 25-hydroxyvitamin D and colon cancer: eight-year prospective study. Lancet 1989; 2: 1176-1178. DOI: https://doi.org/10.1016/s0140-6736(89)91789-3
6. Giovannucci E. Vitamin D status and cancer incidence and mortality. Adv Exp Med Biol 2008; 624:31–42. DOI: https://doi.org/10.1007/978-3-030-46227-7_3
7. Garland CF, Gorham ED, Mohr SB, Grant WB, Giovannucci EL. Vitamin D and prevention of breast cancer: pooled analysis. J Steroid Biochem Mol Biol 2007; 103:708–711. DOI: https://doi.org/10.1016/j.jsbmb.2006.12.007
8. Garland CF, Garland FC, Gorham ED, Lipkin M, Newmark H. The role of vitamin D in cancer prevention. Am. J. Public Health 2006; 96:252–261. DOI: https://doi.org/10.2105/AJPH.2004.045260
9. Grant W. A review of the evidence supporting the vitamin D-cancer hypothesis in 2017. Anticancer Res 2018; 38:1121-1136. DOI: https://doi.org/10.21873/anticanres.12331
10. Bikle D. Vitamin D Metabolism, Mechanism of Action, and Clinical Applications. Chem Biol 2014; 21(3): 319–329. DOI: https://doi.org/10.1016/j.chembiol.2013.12.016
11. Mahendra A, Karishma, Choudhury BK, Sharma T, Bansal N, Bansal R, Gupta S. Vitamin D and gastrointestinal cancer. J Lab Physicians 2018; 10(1):1-5. DOI: https://dx.doi.org/10.4103%2FJLP.JLP_49_17
12. Dou R, Ng K, Giovannucci E, Manson JE, Qian R, Ogino S. Vitamin D and Colorectal Cancer: Molecular, Epidemiological, and Clinical evidence. Br J Nutr 2016; 115: 1643–1660. DOI: https://doi.org/10.1017/S0007114516000696
13. Ng K, Meyerhardt JA, Wu K, Feskanich D, Hollis BW. Circulating 25-hydroxyvitamin D levels and survival in patients with colorectal cancer. J Clin Oncol 2008; 26:2984–2991. DOI: https://doi.org/10.1200/JCO.2007.15.1027
14. Morales-Oyarvide V, Meyerhardt JA, Ng K. Vitamin D and physical activity in patients with colorectal cancer: Epidemiological Evidence and Therapeutic Implications. Cancer J 2016; 22(3):223-231. DOI: https://doi.org/10.1097/PPO.0000000000000197
15. Maalmi H, Walter V, Jansen L, Chang-Claude J, Owen RW, Ulrich A, Schöttker B, Hoffmeister M, Brenner H. Relationship of very low serum 25-hydroxyvitamin D3 levels with long-term survival in a large cohort of colorectal cancer patients from Germany. Eur J Epidemiol. 2017; 32(11):961-971. DOI: https://doi.org/10.1007/s10654-017-0298-z
16. Wesselink E, Bours MJL, de Wilt JHW, Aquarius M, Breukink SO, Hansson B, Keulen ETP, Kok DE, van den Ouweland J, van Roekel EH, Snellen M, Winkels R, Witkamp RF, van Zutphen M, Weijenberg MP, Kampman E, van Duijnhoven FJB. Chemotherapy and vitamin D supplement use are determinants of serum 25-hydroxyvitamin D levels during the first six months after colorectal cancer diagnosis. J Steroid Biochem Mol Biol 2020; 199:105577. DOI: https://doi.org/10.1016/j.jsbmb.2020.105577
17. Klampfer L. Vitamin D and colon cancer. World J Gastrointest Oncol. 2014; 15; 6(11):430-437. DOI: https://doi.org/4251/wjgo.v6.i11.430
18. Wu G, Xue M, Zhao Y, Han Y, Zhang S, Zhang J, Li C, Xu J. Low circulating 25-hydroxyvitamin D level is associated with increased colorectal cancer mortality: a systematic review and dose-response meta-analysis. Biosci Rep 2020; 31;40(7). DOI: https://doi.org/10.1042/BSR20201008
19. Costantini L, Molinari R, Farinon B, Merendino N. Retinoic Acids in the treatment of most lethal solid cancers. J Clin Med. 2020; 28;9(2):360. DOI: https://doi.org/10.3390/jcm9051346
20. Zhu J, Shi XG, Chu HY, Tong JH, Wang ZY, Naoe T, Waxman S, Chen SJ, Chen Z. Effect of retinoic acid isomers on proliferation, differentiation and PML relocalization in the APL cell line NB4. Leukemia. 1995;9(2):302-309.
21. Li M, Sun Y, Guan X, Shu X, Li C. Advanced progress on the relationship between RA and its receptors and malignant tumors. Crit Rev Oncol Hematol 2014;91(3):271-282. DOI:

https://doi.org/10.1016/j.critrevonc.2014.04.001

22. Nguyen PH, Giraud J, Staedel C, Chambonnier L, Dubus P, Chevret E, Bœuf H, Gauthereau X, Rousseau B, Fevre M, Soubeyran I, Belleannée G, Evrard S, Collet D, Mégraud F, Varon C. All-trans retinoic acid targets gastric cancer stem cells and inhibits patient-derived gastric carcinoma tumor growth. Oncogene. 2016; 35(43):5619-5628. DOI: https://doi.org/10.1038/onc.2016.87
23. Najafzadeh N, Mazani M, Abbasi A, Farassati F, Amani M. Low-dose all-trans retinoic acid enhances cytotoxicity of cisplatin and 5-fluorouracil on CD44(+) cancer stem cells. Biomed Pharmacother 2015; 74:243-251. DOI: https://doi.org/10.1155/2015/624627
24. Applegate CC, Lane MA. Role of retinoids in the prevention and treatment of colorectal cancer. World J Gastrointest Oncol 2015; 7:184-203. DOI: https://doi.org/10.4251/wjgo.v7.i10.184
25. Doldo E, Costanza G, Agostinelli S, Tarquini C, Ferlosio A, Arcuri G, Passeri D, Scioli MG, Orlandi A. Vitamin A, cancer treatment and prevention: the new role of cellular retinol binding proteins. Biomed Res Int 2015; 2015:624627. DOI: https://doi.org/10.1155/2015/624627
26. Lin G, Zhu S, Wu Y, Wang W, Zhang Y, Chen Y, He Z. ω-3 free fatty acids and all-trans retinoic acid synergistically induce growth inhibition of three subtypes of breast cancer cell lines. Sci Rep 2017;7, 2929.
27. Mahady GB, Lawal TO, Patel S, Raut N, Wicks S. Combinations of vitamins A, D2 and D3 have synergistic effects in gastric and colon cancer cells. Functional Foods in Health and Disease 2019; 9(12):749-755. DOI: https://doi.org/10.31989/ffhd.v9i12.646
28. Wicks SM, Lawal TO, Raut N, Patel S, Mahady GB. Ergocalciferol induces apoptosis in breast and colon cancer cell lines via caspase 3/7 and 8 and has synergistic effects with cholecalciferol and all-trans-retinoic acid. In: Proceedings of the Functional Foods for Health 2018.
29. Kanabar P, Los N, Abrevia Z, Cline M, Patel S, Lawal TO, Mahady GB. Transcriptomic analysis reveals that combinations of vitamins A, D2 and D3 have synergistic effects in HCT-116 colon cancer cells by altering the expression of genes involved in multiple canonical pathways including apoptosis, regulation of the epithelial mesenchymal transition and immunity. Functional Foods in Health and Disease, 2021; 11(4):154-178. DOI: https://doi.org/10.31989/ffhd.v11i4.784
30. Dobin A., Davis CA, Schlesinger F, Drenkow J, Zaleski C, Jha S, Gingeras TR. STAR: ultrafast universal RNA-seq aligner. Bioinformatics 2013; 29(1):15–21. DOI: https://doi.org/10.1371/journal.pone.0066165
31. Huang Z, Huang D, Ni S, Peng Z, Sheng W. Plasma microRNAs are promising novel biomarkers for early detection of colorectal cancer. Int J Cancer 2010;127: 118–126. Int J Cancer 2010;127: 118-126. DOI: https://doi.org/10.1002/ijc.25007
32. Link A, Balaguer F, Shen Y, Nagasaka T, Lozano JJ. Fecal MicroRNAs as novel biomarkers for colon cancer screening. Cancer Epidemiol Biomarkers Prev 2010;19: 1766–1774. DOI: https://doi.org/10.1158/1055-9965.epi-10-0027
33. Tang JT, Fang JY. MicroRNA regulatory network in human colorectal cancer. Mini Rev Med Chem 2009;9: 921–926. DOI: https://doi.org/10.2174/138955709788681672
34. Liao Y, Smyth GK, Shi W. FeatureCounts: An efficient, general-purpose program for assigning sequence reads to genomic features. Bioinformatics 2014; 30(7): 923–930. DOI: https://doi.org/10.1093/bioinformatics/btt656
35. Soni KK, Meshram D, Lawal TO, Patel U, Mahady GB. Fractions of Boswellia Serrata Suppress LTA4, LTC4, Cyclooxygenase-2 Activities and mRNA in HL-60 cells and reduce lung inflammation in BALB/c Mice. Curr Drug Discov Technol. 2021;18(1):95-104.
36. Schee K, Lorenz S, Worren MM, Gunther C-C, Holden M. Deep Sequencing the MicroRNA Transcriptome in Colorectal Cancer. PLoS ONE 2013;8(6):e66165. DOI: https://doi.org/10.1371/journal.pone.0066165
37. McCarthy DJ, Chen Y, Smyth GK. Differential expression analysis of multifactor RNA-Seq experiments with respect to biological variation. Nucleic Acids Res, 2012; 40(10), 4288–4297. DOI: https://doi.org/10.1093/nar/gks042
38. Fu X, Fu N, Guo S, Yan Z, Xu Y, Hu H, Menzel C, Chen W, Li Y, Zeng R. Estimating the accuracy of RNA-Seq and microarrays with proteomics. BMC Genomics 2009; 10:161. DOI: https://doi.org/10.1186/1471-2164-10-161
39. Bradford JR, Hey Y, Yates T, Li Y, Pepper SD, Miller CJ. A comparison of massively parallel nucleotide sequencing with oligonucleotide microarrays for global transcription profiling. BMC genomics 2010; 11:282-285. BMC genomics 2010; 11:282-285.
40. Benjamini, Y, Hochberg, Y. Controlling the False Discovery Rate: A Practical and Powerful Approach to Multiple Testing. Journal of the Royal Statistical Society. Series B (Methodological), 1995; 57(1): 289–300.
41. Li H, Durbin R. Fast and accurate long-read alignment with Burrows-Wheeler transform. Bioinformatics 2010;26, 589–95.

DOI: https://doi.org/10.1093/bioinformatics/btp698

42. Martin, M., 2011. Cutadapt removes adapter sequences from high-throughput sequencing reads. EMBnetjournal 17 No 1 Gener. Seq. Data Anal. - 1014806ej171200. DOI: https://doi.org/10.14806/ej.17.1.200
43. McCarthy DJ, Chen Y., Smyth GK. Differential expression analysis of multifactor RNA-Seq experiments with respect to biological variation. Nucleic Acids Res 2012;40: 4288–97. DOI: https://doi.org/10.1093/nar/gks042
44. Bland JM, Altman DG. Statistical methods for assessing agreement between two methods of clinical measurement. Lancet. 1986;327 (8476): 307–10.
45. Bland JM, Altman DG. Measuring agreement in method comparison studies. Statistical Methods in Medical Research. 1999; 8 (2): 135–60.
46. Kramer A, Green J, Pollard J, Tugendrich S. Causal analysis approaches in Ingenuity Pathway Analysis. Bioinformatics 2014; 30:523-530.
47. Liu Y, Bodmer W. Analysis of P53 mutations and their expression in 56 colorectal cancer cell lines PNAS 2006; 103;976-981. DOI: https://doi.org/10.1073/pnas.0510146103
48. PTEN mRNA NIH Primer Blast, 2020
49. Florio M, Hernandez MC, Yang H, Shu HK, Cleveland JL, Israel MA. Id2 promotes apoptosis by a novel mechanism independent of dimerization to basic helix-loop-helix factors. Mol Cell Biol. 1998;18(9):5435-5444. Mol Cell Biol. 1998;18(9):5435-5444. DOI: https://doi.org/10.1128/mcb.18.9.5435
50. NIH Primer BLAST: www.accessed June, 15 2021.
51. Muto A, Kizaki M, Yamato K, Kawai Y, Kamata-Matsushita M, Ueno H, Ohguchi M, Nishihara T, Koeffler HP, Ikeda Y. 1,25-Dihydroxyvitamin D3 induces differentiation of a retinoic acid-resistant acute promyelocytic leukemia cell line (UF-1) associated with expression of p21(WAF1/CIP1) and p27(KIP1). Blood 1999; 93(7):2225–2233.
52. Volinia S, Calin GA, Liu CG, Ambs S, Cimmino A, Petrocca F, Visone R, Iorio M, Roldo C, Ferracin M, Prueitt RL, Yanaihara N, Lanza G, Scarpa A, Vecchione A, Negrini M, Harris CC, Croce CM. A microRNA expression signature of human solid tumors defines cancer gene targets. Proc Natl Acad Sci U S A. 2006;14;103(7):2257-2261. Proc Natl Acad Sci U S A. 2006;14;103(7):2257-2261.
53. Chuang KH, Whitney-Miller CL, Chu CY, Zhou Z, Dokus MK, Schmit S, Barry CT. MicroRNA-494 is a master epigenetic regulator of multiple invasion-suppressor microRNAs by targeting ten eleven translocation 1 in invasive human hepatocellular carcinoma tumors. Hepatology. 2015;62(2):466-80. DOI: https://doi.org/10.1002/hep.27816
54. Lin WD, Zou Heng, Mo, Chong J, Jiang H, Yu CY, Jiang Z, Yang Y, He B, Wang K. Micro1278 Leads to Tumor Growth Arrest, Enhanced sensitivity to oxaliplatin and vitamin D and inhibits metastasis via KIF5B, CYP24A1, and BTG2, respectively. Frontiers in Oncology 2021;11: DOI: https://doi.org/10.3389/fonc.2021.637878
55. Liu W, Song Y, Zhang C, Gao P, Huang B. The protective role of all-trans-retinoic acid (ATRA) against colorectal cancer development is achieved via increasing miR-3666 expression and decreasing E2F7 expression. Biomed Pharmacother. 2018;104:94–101. DOI: https://doi.org/10.1016/j.biopha.2018.05.015
56. Wang Z, Jiang Y, Guan D, Li J, Yin H, Pan Y. Critical Roles of p53 in Epithelial-Mesenchymal Transition and Metastasis of Hepatocellular Carcinoma Cells. PLoS ONE 2016;8(9): e72846. DOI: https://doi.org/10.1371/journal.pone.0072846
57. Lee, YR, Chen M, Pandolfi PP. The functions and regulation of the PTEN tumour suppressor: new modes and prospects. Nat. Rev. Mol. Cell Biol. 2018; 19, 547–562. DOI: https://doi.org/10.1038/s41580-018-0015-0
58. Li H, Yang BB. Stress response of glioblastoma cells mediated by miR-17-5p targeting PTEN and the passenger strand miR-17-3p targeting MDM2. Oncotarget 2012; 3:1653–1668.
59. Stoen MJ, Andersen S, Rakaee M. High expression of miR-17-5p in tumor epithelium is a predictor for poor prognosis for prostate cancer patients. Sci Rep 2011; 11: 13864.
60. Li B, Lu Y, Wang H, Han X, Mao J, Li J, Yu L, Wang B, Fan S, Yu X. miR-221/222 enhance the tumorigenicity of human breast cancer stem cells via modulation of PTEN/Akt pathway. Biomed. Pharmacother. 2016;79: 93–101.
61. Schetter AJ, Leung SY, Sohn JJ, et al. MicroRNA expression profiles associated with prognosis and therapeutic outcome in colon adenocarcinoma. JAMA. 2008;299(4):425-436.
62. Zhao Q, Chen S, Zhu Z.. miR-21 promotes EGF-induced pancreatic cancer cell proliferation by targeting Spry2. Cell Death Dis 2018;9: 1157. DOI: https://doi.org/10.1038/s41419-018-1182-9
63. Wu Y, Song Y, Xiong Y, Wang X, Xu K, Han B, Bai Y, Li L, Zhang Y, Zhou L: MicroRNA-21 (Mir-21) Promotes Cell Growth and Invasion by Repressing Tumor Suppressor PTEN in Colorectal Cancer. Cell Physiol Biochem 2017;43:945-958. DOI: https://doi.org/10.1159/000481648
64. Paolella BR, Havrda MC, Mantani A, Wray CM, Zhang Z, Israel

MA. p53 directly represses Id2 to inhibit the proliferation of neural progenitor cells. Stem Cells. 2011;29:1090–101.

65. Rockman SP, Currie SA, Ciavarella M, Vincan E, Dow C, Thomas RJ, Phillips WA. Id2 is a target of the beta-catenin/T cell factor pathway in colon carcinoma. J Biol Chem. 2001;276:45113–119.
66. Linder P, Jankowsky E. From unwinding to clamping — the DEAD box RNA helicase family. Nat. Rev. Mol. Cell Biol. 2011;12, 505–516. DOI: https://doi.org/10.1038/nrm3154
67. Chen HJ, Wei Z, Sun J, Bhattacharya A, Savage DJ, Serda R, Mackeyev Y, Curley SA, Bu P, Wang L, Chen S, Cohen-Gould L, Huang E, Shen X, Lipkin SM, Copeland NG, Jenkins NA, Shuler ML. A re-cellularized human colon model identifies cancer driver genes. Nat Biotechnol. 2016;34(8):845-51.
68. Cai Q, Guo Y, Xiao B, Banerjee S, Saha A, Lu J. Epstein-Barr virus nuclear antigen 3C stabilizes Gemin3 to block p53-mediated apoptosis. PLoS Pathog. 2011;7, e1002418. PLoS Pathog. 2011;7, e1002418